JOURNAL OF GEOPHYSICAL RESEARCH, VOL. 100, NO. D2, PAGES 2905–2926, FEBRUARY 20, 1995

Evaluation of the potential impact of methane clathrate destabilization on future global warming

L.D. Danny Harvey and Zhen Huang[1]

Department of Geography, University of Toronto, Toronto, Ontario, Canada

Abstract. Future global warming due to anthropogenic emissions of greenhouse gases has the potential to destabilize methane clathrates, which are found in permafrost regions and in continental slope sediments worldwide, resulting in the release of methane gas. Since methane is a strong greenhouse gas, this could produce a potentially important positive feedback. Here, the coupled heat transfer and methane destabilization process in oceanic sediments is modeled in a series of one-dimensional, vertical columns on a 1° x 1° global grid. Terrestrial permafrost is divided into 11 columns based on mean annual surface air temperature. Our base case clathrate distribution results in about 24,000 Gt C as methane clathrate in marine sediments and about 800 Gt C in terrestrial sediments, only a small fraction of which could be destabilized by future global warming. Scenarios of anthropogenic CO_2 and CH_4 emission are used to drive a simple model of the carbon cycle, yielding scenarios of CO_2 and CH_4 concentration increase. These increases drive a one-dimensional coupled atmosphere-ocean climate model. Globally averaged temperature changes as a function of time and ocean depth are used as upper boundary conditions to drive the heat transfer/methane clathrate release models. Three versions of the ocean model are used which result in different temperature perturbations at the sediment-water interface: a purely diffusive ocean model, an upwelling-diffusion ocean model with fixed temperature of bottom water formation, and an upwelling-diffusion ocean model with a feedback between surface temperature and the upwelling velocity. Methane release from clathrate destabilization is added to the anthropogenic CH_4 emission, leading to stronger increases in both CH_4 and CO_2 concentration. Based on a wide variety of parameter input assumptions and anthropogenic emission scenarios, it appears that the potential impact on global warming of methane clathrate destabilization is smaller than the difference in warming between low and medium, or medium and high anthropogenic CO_2 emission scenarios, or arising from a factor of two variation in climate sensitivity. Global warming increases by 10-25% compared to the case without clathrate destabilization for our scenarios using what, in many respects, are worst case assumptions.

Introduction

Clathrates are icelike compounds formed when water freezes in the presence of sufficient methane and other gases, such that these gases become trapped within the water molecule lattice. Over 99% of the naturally occurring clathrates are methane clathrates. Clathrates are stable over a limited range of temperatures and pressures found in sediments under permafrost regions and in the ocean, but some clathrates could be destabilized as a result of climatic warming induced by the current buildup of greenhouse gases, thereby releasing potentially large amounts of methane to the atmosphere and amplifying the warming.

Analysis of potential climate-methane clathrate feedback is beset by enormous uncertainties, the most important being extremely scant knowledge of the total amount of clathrate and its distribution. *Kvenvolden et al.* [1993] compiled evidence concerning the distribution of marine clathrate. Methane clathrates have been recovered from ocean sediment cores in 14 different areas of the world, and geophysical and geochemical evidence for them has been found for 33 other areas. Table 1 summarizes estimates of the total amount of methane carbon in clathrates, which span 3 orders of magnitude. For a geothermal gradient greater than 14 K km^{-1}, the average surface temperature must be less than 0°C for methane clathrate to be stable at any depth [*MacDonald*, 1990]. As geothermal gradients on land exceed this value, terrestrial clathrates can occur only in permafrost regions. On outer continental shelves and slopes the pressure-temperature conditions at the sediment-water interface are such that methane clathrates can exist for depths of 250 to several hundred meters in parts of all latitude zones.

Estimates of the amount of methane that would be released by global warming also differ widely. *Revelle*

[1]Permanently at Institute of Atmospheric Physics, Chinese Academy of Sciences, Beijing.

Paper number 94JD02829.
0148-0227/95/94JD-02829$05.00

Table 1. Estimates of the Global Volume and Methane Content of Terrestrial and Oceanic Methane-Clathrate Reservoirs According to Various Authors

Terrestrial		Oceanic		Reference
10^{13} m^3	Gt C	10^{13} m^3	Gt C	
5.7	31.3	500-2500	2750-13700	*Trofimuk et al* [1977]
3.1	17.0	3100	17000	*McIver* [1981]
3400	18681	760000	4176000	*Dobrynin et al* [1981]
1.4	7.6			*Meyer* [1981]
10	54.9	1000	5500	*Makogon* [1988]
		1800	9890	*Kvenvolden* [1988]
73.7	400	2000	11000	*MacDonald* [1990]

[1983] estimated that 0.64 Gt methane (0.48 Gt C) would be released per year following a CO_2 doubling, based on the assumption that a 100-m-thick clathrate layer on continental slopes worldwide would be destabilized. Given an atmospheric methane residence time of at least 12 years (based on recent revisions in the inferred tropospheric OH concentration and in the CH_4-OH rate constant, as discussed by *Harvey* [1993a]), this would give a steady state methane increase of at least 5.8 Gt C, more than doubling the present atmospheric inventory of 3.6 Gt C. *Chamberlin et al.* [1983] estimated that a 1°C global warming would lead to the release of 90 Gt methane over a period of several decades. For an exponentially increasing surface temperature increase which reaches 5.5° by 2050, *MacDonald* [1990] estimates that 3 Gt C would be released over a 200-year period from permafrost regions but does not consider potential releases from oceanic sediments. *Kvenvolden* [1988] concluded that potential methane releases from permafrost and oceanic regions over the next century are likely to be small and their climatic impact minimal. Nevertheless, concerns still remain concerning the potential impact of climate-clathrate feedback [*Lashof*, 1989; *Leggett*, 1990].

This paper reexamines the question of the potential role of methane clathrate destabilization in future global warming induced by anthropogenic greenhouse gas increases. We utilize a modeling framework which involves solving for heat conduction, methane clathrate destabilization, and subsequent upward movement of destabilized methane in 11 vertical columns representing permafrost regions with different surface temperatures and about 2000 1° x 1° columns at oceanic grid points where the ocean depth and bottom temperature are such that methane clathrate could be destabilized and released to the atmosphere. In the first part of our investigation the terrestrial and oceanic columns are driven by a series of step-function temperature increases at the surface (land case) or at the sediment-water interface (ocean case). The methane flux to the atmosphere, the increase in methane concentration, the production of atmospheric CO_2 by methane oxidation, the gradual removal of the CO_2 by oceanic uptake, and the surface-troposphere heating perturbation due to the methane and CO_2 increases are computed. In the second part of the study, a slightly modified version of the coupled one-dimensional climate-carbon cycle model of *Harvey* [1989a] is used to generate scenarios of time-dependent, globally averaged temperature increase at the surface and as a function of ocean depth. These temperature perturbations are used to drive the methane release submodels, with the methane release and subsequent CO_2 production added to the anthropogenic methane and CO_2 production, thereby providing a feedback. A range of anthropogenic emission scenarios, climate model sensitivities, and ocean model formulations is considered in this investigation.

Our purpose in this modeling exercise is not to make predictions concerning the future impact of methane clathrate destabilization, because the enormous uncertainties render any prediction meaningless. Rather, we wish to set reasonable upper bounds for worst case scenarios and to compare the impact on future warming of the worst case scenario with the impact of other sources of uncertainty. We also wish to identify the most important requirements for new data and to establish a modeling framework which will permit improved estimates of the limiting worst case scenario as more data become available.

Processes of Methane Release

The processes and timescales involved in methane release from permafrost regions and from oceanic sediments are distinctly different. Figure 1 illustrates the variation in the critical temperature for methane clathrate destabilization as a function of depth. Also shown is a representative temperature profile in permafrost regions. Given a mean annual surface temperature of -10°C and a typical temperature gradient of 20 K km^{-1}, the upper boundary of the stable zone will be at a depth D of about 200 m. Given a thermal diffusivity K_T of the order of 10^{-6} m^2 s^{-1}, the time scale for penetration of a thermal anomaly to depth D is $D^2/K_T \sim 10^3$ years. Thus significant methane release from permafrost regions would not occur for several centuries. As surface temperature warming propagates downward, the temperature profile may eventually become tangent to the phase boundary curve. *MacDonald* [1990] suggested that when this occurs, all of the destabilized methane below the tangent point would be free to migrate to the surface, although the timescale for this process is of the order of thousands of years. However, this could be inhibited by the presence of ice in the permafrost region above the destabilized clathrate as long as the permafrost has not completely melted. A permafrost layer about 250 m thick would still exist after complete destabilization of the clathrate layer shown in Figure 1 had occurred and would require an additional surface warming of about 5°C before it completely melted.

In oceanic sediments, three different relationships between the clathrate-stable zone and sediment-water interface can occur. In the first case, illustrated in Figure 2a, the top boundary of the stable zone occurs below the sediment-water interface. Also shown in Figure 2a is the depth z_{max} at which the difference ΔT_{cr} between the sediment temperature and the destabilization temperature is maximized. In the remaining two cases the top of the stability zone occurs above the sediment-water interface. In case 2 (Figure 2b) the sediment-water interface occurs above z_{max}, while in case 3 (Figure 2c) it occurs below z_{max}.

The timescale for penetration of surface warming to the sediment-water interface ranges from a few years (in areas of

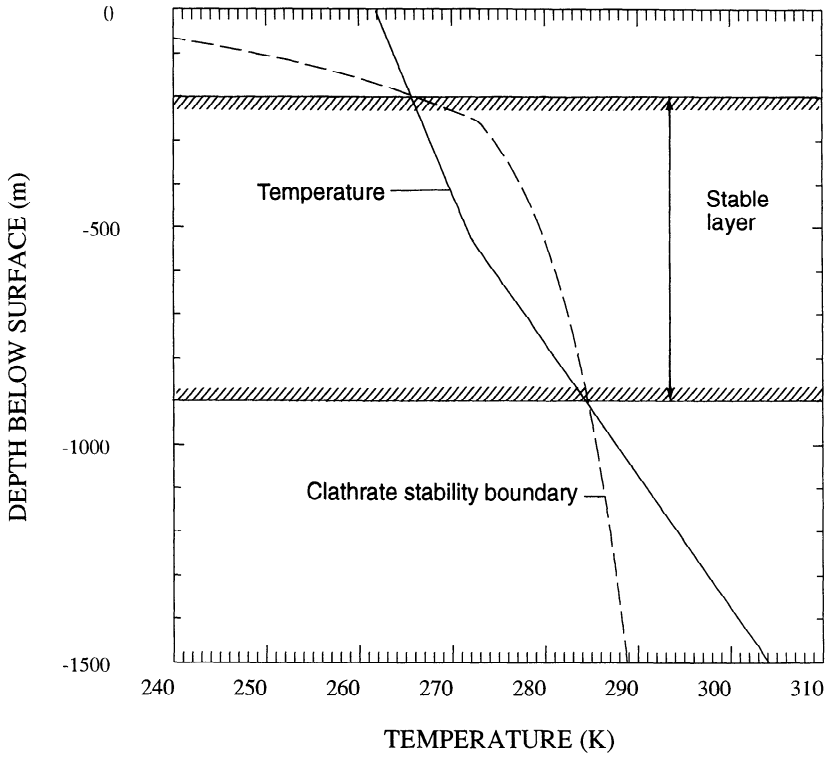

Figure 1. Variation with depth of the stability boundary for pure methane-clathrate and a typical temperature profile in permafrost regions.

deep convection) to at most a few decades. For columns where the upper boundary of the stable zone occurs below the sediment-water interface, the timescale for clathrate destabilization is dependent on the sediment thermal diffusivity and depth of the stable zone below the sediment surface. Since these are of the same order of magnitude as the values appropriate for land columns and there is large uncertainty in the amount of terrestrial clathrate, we neglect case 1 ocean columns (only 47 such cases occur on a 1° x 1° grid). In case 2 columns, destabilization occurs first in the region immediately below the sediment-water interface and progresses downward; destabilized methane in this region will be quickly released to the seawater. Later, as the thermal wave penetrates downward, destabilization at the bottom of the stable zone will also occur (see Figure 2b). In case 3 ocean columns, destabilization begins at the bottom of the stable zone, once the warming has penetrated to this depth, and progresses upward (see Figure 2c).

Claypool and Kaplan [1974] present a representative H_2O-CH_4 phase diagram in the pressure-CH_4 concentration plane, while *Hyndman and Davis* [1992] give a phase diagram in the temperature-CH_4 concentration plane. As methane is released from clathrate destabilization due to warming, bubbles will form, although they can be expected to be very small and finely disseminated at the beginning. The bubbles, having negligible density compared to that of water, would tend to move upward under a strong buoyancy force, although air bubbles in gas wells have been observed to completely plug fine-grained sediments due to strong adhesive forces on the bubble surface preventing its deformation. Clathrates have been observed in sediments ranging from silty clays [*Tucholke et al.* 1977] to coarse clastic sedimentary wedges [*Hyndman and Davis*, 1992]. The process of methane release to the atmosphere is a complex, multiphase fluid flow problem involving a sediment-gas-water system. It seems most appropriate to represent the upward movement of methane bubbles as an advective rather than a diffusive process. *Freeze* [1979] indicates a typical pore water advection velocity in fractured sediment of 10^{-7} m s^{-1}. As long as sediment pores are not plugged, we expect a substantially faster velocity of methane bubbles due to their buoyancy. However, our results are insensitive to the advection velocity as long as it is 10^{-6} m s^{-1} or larger, so we adopt a value of 10^{-6} m s^{-1} here.

In instances on continental slopes where methane clathrates are destabilized at the bottom of the stable zone, we can envisage one of three things happening: (1) If the overlying stable layer does not impede vertical movement of bubbles, the bubbles will migrate into the stable zone. If the rate of migration is slow enough that thermal equilibrium between the bubble and its surroundings applies, the methane will refreeze as clathrate and warm the stable layer, bringing it closer to the clathrate melting point. (2) If the overlying stable zone is impermeable, then pressure will build up in destabilized layers where the destabilized methane tends to occupy a greater volume than the original clathrate. Since 1 m^3 of pure methane clathrate occupies 170.7 m^3 at STP upon destabilization, and pressure increases by about 1 atm for every 10-m depth, an expansion tendency and associated pressure increase would occur when clathrate destabilizes at depths below sea level of less than about 1700 m (depending on temperature). A large enough pressure buildup would

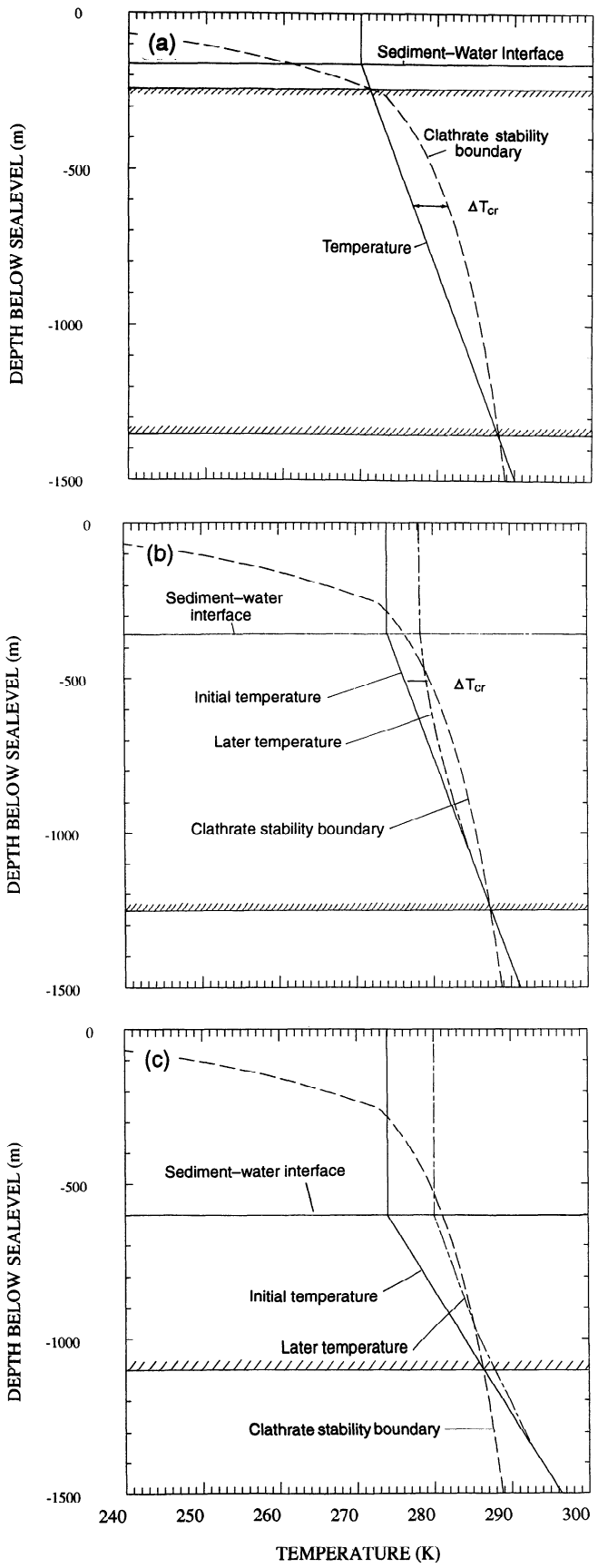

Figure 2. Relationship between the sediment-water interface, the stable clathrate zone, and $(\Delta T_{cr})_{max}$ in marine sediments for (a) case 1, (b) case 2, and (c) case 3 (see text).

induce fracturing of the overlying sediment and rapid release of some of the underlying methane. (3) Even when the overlying stable zone is not completely impermeable, a buildup of methane gas could reduce the bulk sediment shear strength which, in areas of sloping sediments, could lead to downslope movement and rapid release of most or all of the destabilized methane. This is inferred to have occurred at a number of sites [*Carpenter*, 1981; *McIver*, 1982; *Kayen*, 1988]. *Paull et al.* [1991] incorporated this possibility by assuming that 1% of the methane below the stable zone in marine sediments is released per year. We explicitly consider the first two possibilities here, since the uncertainty in fracture release can be taken to include possible additional releases due to sediment slumping.

Once methane bubbles reach the sediment-water interface, the buoyancy force would tend to rapidly propel the bubbles to the atmosphere. However, some dissolution of the bubbles would occur during transit, even where the water is supersaturated with respect to atmospheric methane. Data summarized by *Hovland et al.* [1993] indicate that a methane bubble 2 mm in diameter at 100 m depth will completely dissolve just as it reaches the surface, whereas 15% of a 1-cm bubble released at 300 m will reach the surface. Once methane dissolves, upward transport by turbulent diffusive mixing along a gradient of decreasing concentration would occur, followed by ocean-to-air gas transfer driven by the mixed layer-atmosphere partial pressure difference, with a characteristic timescale of years.

Oxidation of dissolved methane could also reduce the methane flux to the atmosphere. Anaerobic methane oxidation occurs in the sulfate-reducing zone found at the top of the sediment column and in anoxic waters, while aerobic oxidation occurs in oxygenated waters. At Kattegat (Denmark) and Saanich Inlet (Canada), complete oxidation of upward dissolved methane fluxes of 0.03-0.04 μmol cm^{-2} yr^{-1} and 9-90 μmol cm^{-2} yr^{-1}, respectively, occurs in the sulfate-reducing zone at the top of the sediment column [*Iverson and Jorgensen*, 1985; *Devol*, 1993]. This oxidation zone is likely to be largely bypassed if methane is transported upward as bubbles [*Martens and Klump*, 1980; *Chanton and Martens*, 1988]. Measured aerobic oxidation rates in the water column vary by several orders of magnitude. In Saanich Inlet an upward methane flux from anoxic waters (at 140-m depth) of about 1.4 μmol cm^{-2} yr^{-1} was observed to be completely oxidized in the aerobic zone [*Ward et al.*, 1989], while in the Cariaco Basin (off Venezuela), only about 5% of an upward flux of 2 μmol cm^{-2} yr^{-1} at 280-m depth was observed to be oxidized [*Ward et al.*, 1987]. About 90% of the methane released from the columns in our simulations occurs at a flux density greater than 3 μmol cm^{-2} yr^{-1}, and about 50% occurs at a density greater than 6 μmol cm^{-2} yr^{-1}, which is somewhat larger than for the two cases reported above. The critical issue is whether clathrate decomposition will release methane faster than it can be consumed in the water column.

Given uncertainties in the fraction of methane released from marine sediments which would be oxidized before reaching the atmosphere and our desire to construct a worst case scenario, we assume that neither dissolution nor oxidation of the methane released to ocean water significantly reduces the flux to the atmosphere. We also neglect possible oxidation of methane released from permafrost

regions, although oxidation of methane produced in the seasonally thawed surface layer appears to significantly reduce the methane flux to the atmosphere [*Rasmussen et al.*, 1993], while replacing it with a CO_2 flux. However, we assume that no methane is released from permafrost regions until the mean annual surface temperature has warmed to -1°C. Since destabilization of at least the upper part of terrestrial clathrate zones will have occurred before this surface temperature threshold is reached, significant quantities of free methane could accumulate below the permafrost zone, leading to very large upward fluxes once the permafrost completely melts. If this occurs, then a significant fraction of the destabilized methane in permafrost regions might be able to reach the atmosphere without being oxidized. The results presented in this paper are nevertheless worst case scenarios in this respect.

Potential Size of the Methane Clathrate Reservoir

Estimation of the amount of methane worldwide in methane clathrates requires a knowledge of the volume of the clathrate-stable zone, the fraction of the stable volume which contains clathrate, and the fraction of gas sites within the water lattice which contains methane. Determination of the worldwide volume of the clathrate-stable zone in turn requires a knowledge of the variation of the stability boundary and temperature as a function of depth at a fine enough horizontal resolution to allow an accurate global integration. We discuss each of these required data below.

Variation of Stability Boundary With Depth

Theoretical determination of the clathrate phase boundary on a temperature-pressure plane is in agreement with laboratory experiments using pure water [*Sloan*, 1990]. However, water in sediments may contain alcohols or salts, which shift the phase boundary toward the stable region, thereby making methane clathrate more difficult to form, or may contain heavy molecules such as CO_2, NO_3, propane, and hydrogen sulphide, the inclusion of which shifts the phase boundary to the free CH_4 gas side and makes methane clathrate easier to form. Most research on methane clathrate uses the phase boundary for pure water on the grounds that the temperature decrease caused by salts is approximately offset by the temperature increase caused by hydrocarbons heavier than methane [*Kvenvolden and McMenamin*, 1980]. However, other factors might invalidate this assumption. As clathrates form in saline water, salts are excluded, producing a brine with salinities as high as 26% and displacing the phase boundary by over 13 K [*de Roo et al.*, 1983]. Although biologically produced methane contains very little heavy hydrocarbons, thermogenic methane (originating from the Earth's interior) includes enough heavy hydrocarbons to increase its stability range by several hundred meters [*Sloan*, 1990]. The pressure required to form clathrate in porous media is greater than that in a free liquid by as much as 70 kg cm^{-2} [*Sloan* 1990], corresponding to a depth of 700 m for matrix-supported sediments (ie., sediments in which that weight of sediment is entirely supported by grain-to-grain contact, so that the pore water pressure is proportional to depth times water density). Finally, the presence of clay can raise the phase boundary temperature by as much as 3 K in tetrahydrofuran, which is regarded as a suitable analog for normal gas clathrates [*Rueff and Sloan*, 1985].

Makogon [1981] investigated the empirical clathrate stability range for different gas fields and found that the critical conditions statistically converged to that for a pure CH_4-H_2O system. Thus in spite of the potential for large errors at any given location we also adopt the phase boundary for a pure CH_4-H_2O system. The phase boundary can be represented analytically by [*Makogon*, 1981]:

$$\log P = \begin{cases} 5.6414 - 1154.61/T_{cr} & 262K \le T_{cr} \le 273K \\ 1.415 + 0.0417(T_{cr} + 0.01T_{cr}^2) & 0°C \le T_{cr} \le 23°C \\ 1.602 + 0.0428T_{cr} & 24°C \le T_{cr} \le 47°C \end{cases} \quad (1)$$

where P is in atm and T_{cr} is the temperature of the stability boundary.

Variation of Temperature With Depth

Given the mean annual surface temperature in regions of continental permafrost, or the water-sediment interface temperature at the ocean floor, the presence or absence of a clathrate-stable zone and its thickness depend strongly on the vertical temperature gradient. *Lachenbruch et al.* [1987] reports geothermal gradients in cold regions of 16 to 53 K km^{-1}, while *Makogon* [1981] suggests a gradient of 100 K km^{-1} for continental shelf sediments at a depth of 1000 to 3000 m and *Lee and Clark* [1966] suggest a mean gradient on continental shelves of 40 K km^{-1}. *MacDonald* [1990] assumed a gradient of 16.2 K km^{-1} in frozen sediments and 31.2 K km^{-1} in nonfrozen sediments.

Here, we specify temperature as an upper boundary condition and the geothermal heat flux as a lower boundary condition. The steady state geothermal gradient is then determined by the assumed thermal conductivity. Vertically uniform thermal conductivities for clathrate-free marine sediments in each column are taken from the thermal conductivity map of *Louden* [1989], while conductivities for unfrozen and frozen, clathrate-free terrestrial sediments of 1.76 and 3.39 W m^{-1} °C^{-1}, respectively, are adopted here from *MacDonald* [1990]. A thermal conductivity of 0.5 W m^{-1} °C^{-1} is used for pure clathrate, based on *MacDonald* [1990], with the mean thermal conductivity in the clathrate zone given by a proportional weighting of the conductivities for clathrate and clathrate-free sediments. The presence of clathrate results in a greater geothermal gradient due to the low thermal conductivity of clathrate, but a greater gradient results in a thinner stability zone.

We specify a geothermal heat flux of 0.055 W m^{-2} for terrestrial permafrost regions, based on *Lachenbruch* [1982] and other sources, while grid point heat flux values ranging from 0.001 to 0.398 W m^{-2} are specified for the oceanic columns, based on heat flow data of *Louden* [1989]. The resultant steady state temperature gradient ranges from 1.2 to 474°C km^{-1} in marine sediments. However, most temperature gradients are below 100°C km^{-1}, with higher values tending to be a result of local hot spots which might not be representative of an entire grid cell. Therefore we imposed an upper limit on the temperature gradient of 100°C km^{-1},

Table 2. Seafloor Temperature, Depth, and Carbon Content Statistics for All Marine Clathrate Columns Down to a Seafloor Depth of 3000 m

	Max	Min	Ave
Seafloor Temperature, °C	13.8	-1.9	2.3
Seafloor Depth, m	3000	250	2246
Geothermal heat flux, mW m^{-2}	398	1	70.3
Thermal conductivity, W m^{-1} °C^{-1}	4.4	0.5	1.0
Temperature gradient, °C km^{-1}	100	1.2	65.7
Organic carbon content, weight %	2.0	0.25	0.55

which results in an area-weighted mean gradient of 66°C km^{-1} (see Table 2 for this and other results).

Occurrence of Marine Clathrates

Given data for the depth and temperature of the sediment-water interface on a 1° x 1° grid and for sediment thermal conductivity and vertical heat flux and assuming that the laboratory clathrate stability boundary can be used, we calculate a total volume for the marine clathrate-stable zone of 1.65 x 10^{16} m^3 and an average thickness of the stable zone of 277 m. *MacDonald* [1990] assumed an average thickness of 500 m, which leads to an estimated stable zone volume of 3.13 x 10^{16} m^3.

The sediment volume containing methane clathrate is likely to be only a small fraction of the clathrate-stable volume, being limited by the availability of sufficient methane to form methane clathrate. The base of a clathrate layer can produce a horizon on seismic profiles parallel to the ocean bottom and is referred to as a bottom simulating reflector (BSR). BSRs have been identified in many locations worldwide, although not all known or inferred occurrences of clathrates are associated with BSRs [ie., *Harrison and Curiale*, 1982]. When clathrates form, salts are ejected which can be subsequently carried from the site of the clathrate by rising pore fluids [*Hesse and Harrison*, 1981]. If the salt-rich fluids produced at the time of clathrate formation had been removed, then decomposition of clathrate during coring operations will result in lower pore fluid chlorinity, and such dilution is also used to infer the presence of clathrates. In many cases, clathrates have been retrieved from cores; isotopic and chemical analyses indicate that in the vast majority of cases the methane in clathrates is produced from organic matter as a result of biological activity, although in some cases, thermogenic methane, produced at much greater depth, has been identified [*Brooks et al.*, 1984].

Two models have been proposed to explain the presence of clathrates. The first, proposed by *Claypool and Kaplan* [1974] and supported by *Kvenvolden and MacDonald* [1985], postulates that methane forms in situ. Methane is produced only when pore water is depleted in O_2 and sulfate; O_2 is depleted before sulfate, and the depth at which sulfate depletion occurs ranges from a few centimetres to 200 m [*Claypool and Kvenvolden*, 1983]. When the CH_4 concentration exceeds the solubility, clathrates form if the temperature-pressure conditions fall within the stability zone. With ongoing sedimentation, the clathrate zone thickens, and eventually decomposition may occur at the base of the stability zone, producing free gas. An alternative model, proposed by *Hyndman and Davis* [1992], postulates that CH_4 is generated below the stability zone and carried upward into the stability zone by pore fluids as sediments undergo compaction. The large vertical fluid movement needed to produce the inferred clathrate layers can be produced only in thick sedimentary wedges, where deep sea sediments are carried toward continental margins by oceanic crustal plates. BSRs are associated with such environments and are generally restricted to areas where the sediment strata dip landward, which would favor migration of CH_4 along the strata into the stability zone.

The second model implies that clathrates will be concentrated in a relatively thin layer at the base of the stability zone, and this appears to be true in a number of cases. *Hyndman and Davis* [1992] and *Hesse and Harrison* [1981] infer that basal clathrate fills about 50% of the pore space for cases they studied, while *Hyndman and Spence* [1992] infer that clathrate fills 30% of the pore space in a 10 to 30-m-thick basal layer. However, in many cases, clathrate has been recovered from within a few meters of the sediment-water interface [*Yefremova and Zhizhchenko*, 1975; *Brooks et al.*, 1986, 1991; *Ginsburg et al.*, 1992, 1993] or within 20-40 m of the sediment-water interface [*Pflaum et al.*, 1986]. *Ginsburg et al.* [1993] report clathrate filling 30-40% of the sediment volume at a depth of 0.3-1.2 m. Chlorinity data from many sites indicate that clathrate occurs throughout the stability zone. *Hesse and Harrison* [1981], *Kvenvolden and Barnard* [1983], *Kvenvolden and MacDonald* [1985], and *Kvenvolden and Kastner* [1990] report chlorinity profiles in which the chlorinity dilution decreases uniformly from a dilution of 10-50% at the inferred base of the clathrate stability zone to near zero at the sediment-water interface or within a few tens of meters of the sediment-water interface, while *Shipboard Scientific Party* [1990] report a profile with a chlorinity minimum at a 50-m depth. An upward decrease in chlorinity does not imply that the clathrate concentration decreases, however, since a decreasing fraction of the pore fluids produced by progressively shallower (and hence younger) clathrate will have been removed by rising pore water. Hence the chlorinity dilution from decomposition of clathrate during coring operations may decrease as one moves upward within the stability zone even if the clathrate concentration is constant. Nevertheless, clathrate pore concentrations near the tops of these sediment cores probably are lower than the value of 10-50% inferred at the base of the stability zone because they were unable to survive the coring process.

Hesse and Harrison [1981] report chlorinity and organic carbon data from the same cores. Organic carbon decreases steadily from 3% at the sediment surface to 1-2% at the base of the clathrate stability zone in the cores they examined, and this matches a steady decrease in the degree of chlorinity dilution. The degree of chlorinity dilution is consistent with the assumption that the organic carbon content was initially uniform with depth, and that the measured variation is due to an increase with depth in the degree of conversion of organic carbon to methane clathrate. These results clearly implicate in situ formation processes and suggest that in spite of the above arguments the fractional chlorinity dilution is roughly indicative of the fraction of pore space filled with clathrate prior to coring.

Available maps showing the extent of inferred clathrate indicate that clathrates underlie on the order of 10-25% of the seafloor between depths of 250 and 3000 m within a given region [i.e., *Katz*, 1981; *Shipley and Didyk*, 1982; *Kvenvolden and Barnard*, 1983; *Brooks et al.*, 1986, 1991], except for the region of organic-rich sediments in the Beaufort Sea studied by *Kvenvolden and Claypool* [1988], where about 75% of the area is underlain by clathrates. In situ clathrate formation requires a minimum of 0.5% organic carbon [*Kvenvolden and Barnard*, 1983].

Based on the above, we assume the following distribution of clathrate within the stability zone: Using the map of organic carbon content given by *Premuzic et al.* [1982], we eliminate from consideration any columns with less than 0.5% organic carbon. This reduces the potential horizontal extent of clathrate by a factor of 3. Within the remaining columns we assume that 75% of the horizontal area contains clathrate, so that, overall, the horizontal extent of clathrate is 25% of the potential extent for seafloor depths of up to 3000 m. We do not consider columns at seafloor depths greater than 3000 m since very large temperature increases would be required for destabilization. Since clathrate seems to form both by in situ decomposition of organic matter and by upward migration of CH_4 from below the stability zone, we assume that in each column there is a clathrate component which occupies a constant pore fraction with depth and a component which is maximum at the base of the stability zone and decreases with distance above the base. Both components are assumed to exist in every column since we are only interested in replicating possible statistical properties of real distributions. For our base case we assume that the fraction of pore space occupied by clathrate decreases from 20% at the base of the stability zone to 5% at the top of the stability zone. We consider alternative cases in which the pore fraction initially occupied by clathrate varies between 10 and 2½%, or between 40 and 10%. In every case we assume that the sediment porosity decreases exponentially with sediment depth, with a surface porosity of 0.6 and an *e*-folding depth of 1.5 km based on *Davis et al.* [1990]. The three distributions produce total marine clathrate amounts of 12,200, 24,400, and 48,800 Gt C, respectively.

Table 3. Distribution of Methane Clathrate (Gt C) in Marine Sediments With Respect to the Difference $(\Delta T_{cr})_0$ Between Temperature and the Stability Boundary at the Seafloor for the Base Case

$(\Delta T_{cr})_0$	Methane Amount Gt C	Average Depth of Seafloor, m	Average Thickness of Stable Zone, m
0-1	60	395	28
1-2	176	526	72
2-3	77	788	80
3-4	227	785	94
4-5	428	988	136
5-6	314	898	229
6-7	733	1082	172
7-8	349	866	178
8-9	601	1056	254
9-10	719	1008	189
>10	20709	1954	315

A critical parameter governing the release of methane to seawater is the difference $(\Delta T_{cr})_0$ between the temperature of the sediment-water interface and the temperature $(T_{cr})_0$ for destabilization at the interface. In the absence of fracturing which releases destabilized methane from the lower part of the initially stable zone, no methane will be released until the warming at the sediment-water interface exceeds $(\Delta T_{cr})_0$. Table 3 gives the distribution of methane carbon with respect to $(\Delta T_{cr})_0$ for the base case vertical clathrate distribution. Also given in Table 3 is the average seafloor depth and thickness of the stable zone for the columns in each $(\Delta T_{cr})_0$

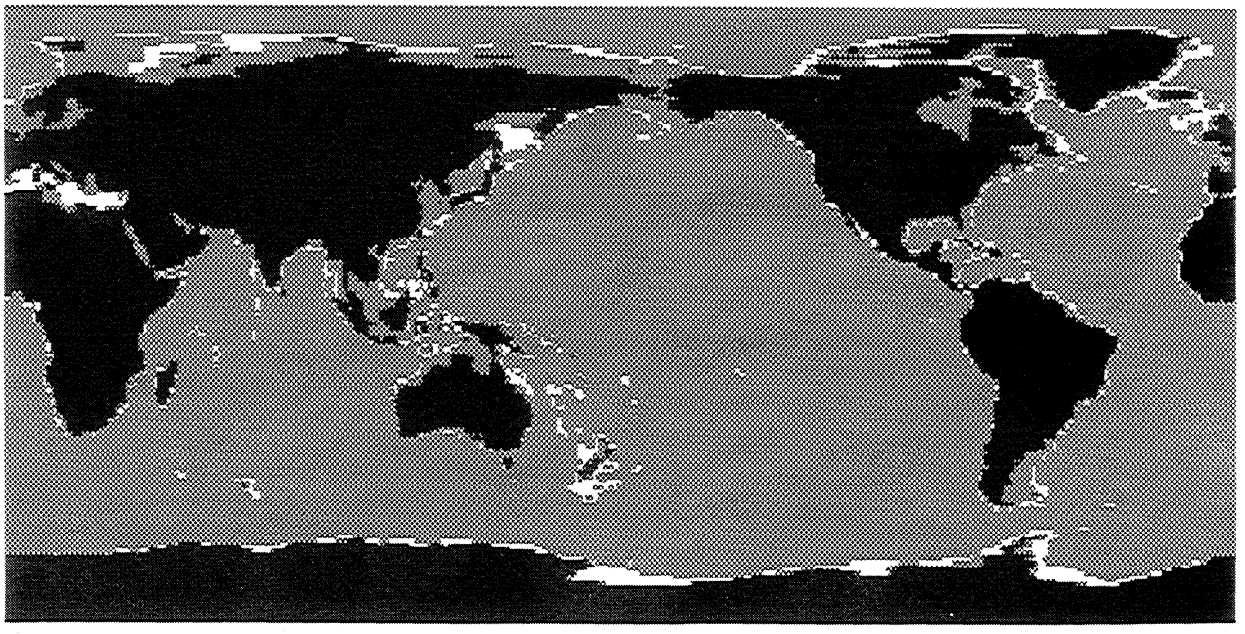

Figure 3. Distribution of marine sediment columns on a 1° x 1° grid where $\Delta T_{cr} < 10$°C at the sediment-water interface.

category. Note that about 98% of the methane clathrate occurs in regions where $(\Delta T_{cr})_0$ is at least 4°C. Thus of the 24,400 Gt C assumed to be present, only 540 Gt C are susceptible to release for warming at the sediment-water interface of up to 4°C, in the absence of fracturing. If the steady state temperature perturbation associated with a greenhouse gas increase diminishes with increasing depth over most of the global ocean, as in the one-dimensional upwelling-diffusion model with fixed upwelling velocity and temperature of bottom water formation, a substantially larger and hence less likely surface warming will be required to destabilize most of the marine methane clathrate. On the other hand, as indicated in Table 3, the columns most susceptible to clathrate destabilization are also the shallowest columns and thus will tend to experience warming sooner than the less susceptible columns. In reality, methane clathrate is probably not distributed throughout the stable volume in the exact manner which we have assumed, but it is still likely that a substantial fraction of oceanic clathrate requires a very large warming at the sediment-water interface for it to be destabilized and released to the atmosphere. Nevertheless, the potential size of the marine clathrate reservoir is so large that even relatively small releases could have a nonnegligible effect on climate.

Figure 3 shows the distribution of 1° x 1° grid squares for which $(\Delta T_{cr})_0 < 10$°C and organic matter content exceeds 0.5%. These grid squares are distributed through all latitudes and ocean basins but are somewhat concentrated at high latitudes. These are the only grid points retained in our simulations, resulting in about 800 marine columns and initial clathrate carbon amounts of 1843, 3686, and 7372 Gt for the three sets of assumptions concerning the pore fraction filled with clathrate.

Finally, we investigated the possible effect of lower sea level during the last ice age on the present-day distribution of marine methane clathrate. A given lowering of sea level is equivalent to shifting the stability boundary downward by the same amount. Table 4 shows the effect of lowering sea level by 150 m on the amount of methane in the columns belonging, prior to sea level lowering, to each of the $(\Delta T_{cr})_0$ categories. As seen from Table 4, a lowering of sea level completely eliminates clathrate from columns which, today, have $(\Delta T_{cr})_0 < 1$°C. For columns with $(\Delta T_{cr})_0 < 4$°C, the amount of clathrate after a 150 m sea level lowering drops from 540 to 112 Gt C. Two factors could have mitigated the reduction in these columns today: cooling of the seafloor at the same time that sea level was lowered and formation of new clathrate since the end of the last ice age. Table 4 shows the effect of sea level lowering on the available clathrate when concurrent seafloor coolings of 2°C and 4°C are imposed, these representing a reasonable range of actual ice age ocean water temperature decreases. The loss of clathrate in the columns with $(\Delta T_{cr})_0 < 4$°C is substantially reduced as a result of cooling concurrent with sea level lowering.

Because of uncertainty concerning both the extent of ice age ocean cooling at the time of maximum sea level drop and the extent of clathrate formation since the end of the last ice age and given our desire to construct a limiting worst-case scenario, we neglect the possible effect on present-day clathrate amounts of lower sea levels during the last ice age.

Table 4. Effect of Lower Sea Level and Colder Conditions During the Last Ice Age and on CH_4 Clathrate Amount for the Base Case Clathrate Distribution

$(\Delta T_{cr})_0$	Initial T	150 m Sea Level Lowering ΔT=0°C	ΔT=-2°C	ΔT=-4°C
0-1	60	0	0	0
1-2	176	1	4	7
2-3	77	18	46	71
3-4	227	93	192	281
0-4	540	112	242	359
> 4	23873	22527	25242	27820

Table 5. Parameters Used in Generating Terrestrial Permafrost Columns, and Properties of These Columns

Input Parameters	Value
Geothermal flux	55 mW m^{-2}
Frozen thermal conductivity	3.39 W m^{-1} °C^{-1}
temperature gradient	16.2 °C Km^{-1}
Unfrozen thermal conductivity	1.76 W m^{-1} °C^{-1}
temperature gradient	31.2 °C Km^{-1}
Total area	8.752 x 10^{12} m^2
Porosity	0.25
Area fraction underlain with clathrate	10%
Pore fraction filled with clathrate	2 1/2%, 5%, or 10%
Total methane	394, 788, or 1576 Gt C

Column Number	T_{sfc} (°C)	Results z_t, m	z_b, m	Thickness, (m)	Gt C
1	-5 to -6	271	476	205	21
2	-6 to -7	252	609	357	31
3	-7 to -8	237	731	494	38
4	-8 to -9	226	824	598	73
5	-9 to -10	216	911	695	80
6	-10 to -11	207	995	788	84
7	-11 to -12	199	1076	877	86
8	-12 to -13	190	1155	965	96
9	-13 to -14	181	1244	1063	95
10	-14 to -15	174	1311	1137	94
11	< -15	167	1393	1226	90
Total					788

Values of z_t and z_b are the depths of the top and bottom of the stability zone and T_{sfc} the surface temperature.

Occurrence of Terrestrial Clathrate

The volume of the clathrate-stable region in permafrost regions in our model depends on the area of the region and the assumed surface temperature, geothermal heat flux, and thermal conductivity, which together determine the tempera-

ture variation as a function of depth. We estimated the northern hemisphere land surface area with mean annual surface air temperature ranging from -5°C to -15°C in 1°C intervals, and colder than -15°C, giving a total of 11 columns. So as to have close to the same horizontal clathrate extent as estimated by *MacDonald* [1990], we assume that 10% of the horizontal area in each temperature class is underlain with clathrate and, for our base case, we assume that 5% of the pore volume in these regions is filled with clathrate at all depths within the stability zone. We assume a porosity for terrestrial sediments of 0.25 at all depths, based on *MacDonald* [1990]. This gives a total terrestrial clathrate reservoir of 788 Gt C for our base case. We also consider cases where 2½ and 10% of the pore space is filled with clathrate, which give terrestrial reservoirs of 394 and 1576 Gt C, respectively. By comparison, *MacDonald* [1990] assumed a terrestrial clathrate reservoir of 400 Gt C. Table 5 summarizes the input assumptions along with the resultant top and bottom depths of the stable zone and methane amounts for each column. The estimated total clathrate amount and its distribution are of course extremely uncertain, and the simulation results presented later are useful for illustrative purposes only.

Model Description

Sediment Heat Diffusion and Methane Release Model

The temperature and free methane distribution for a series of one-dimensional columns is solved, given the governing equations

$$\frac{\partial T}{\partial t} = \frac{\partial}{\partial z}\left(K_T(z)\frac{\partial T}{\partial z}\right) - \left(\frac{L_d}{\rho c_p}\right)q_d \qquad (2)$$

$$\frac{\partial C}{\partial t} = \frac{\partial}{\partial z}(wC) + q_d \qquad (3)$$

where T and C are the temperature and free methane concentration, K_T is the diffusion coefficient for heat, w is the advection velocity of methane bubbles due to their buoyancy, L_d is the methane clathrate dissociation energy, ρ and c_p are the sediment bulk density and specific heat, and q_d is the rate of free methane production (kg s^{-1} m^{-3}) due to dissociation of methane clathrate. If methane is advected upward into the stable zone from the underlying unstable zone, refreezing of methane occurs and $q_d < 0$.

For a typical methane clathrate concentration of 6 kg m^{-3} (corresponding roughly to 10% of the pore space filled with clathrate in sediment with porosity of 50%) and a heat of dissociation for pure methane clathrate of 4.5 x 10^6 J kg^{-1}, the bulk volumetric heat of dissociation is 3 x 10^7 J m^{-3}, which is an order of magnitude greater than the typical bulk sediment heat capacity of 2.1 x 10^6 J m^{-3} °C^{-1}. The volumetric heat of dissociation will therefore largely determine, for a given heat flux convergence, the rate of movement of the stability boundary.

The governing equations are solved in discretized form assuming a uniform grid spacing of 10 m and semi-implicit time differencing with 60-day time steps. The bottom of the model is placed at a depth of 3000 m below sea level. The model is initialized by assuming a given layer to be entirely stable if the temperature in the middle of the layer is colder than the stability boundary at the midlayer depth. If the computed temperature at the end of a time step exceeds the destabilization temperature, the temperature is reset to the critical temperature and the excess heat is used to melt clathrate. In reality, destabilized clathrates do not decompose completely but leave a partial structure which will readily reform clathrate with a temperature decrease [*Makogon*, 1981; *Vysniauskas and Bishnoi*, 1983; *Schroeter* et al., 1983]. The residual structure is stable up to 315 K and the residual population varies inversely with temperature [*Chen*, 1980]. Temperatures within the top 2000 m of sediments are generally below 315 K, so the effect of partial decomposition should, in principle, be included but is neglected here.

The model simulations begin with a steady state temperature profile and the pore water assumed to be saturated with respect to methane in the stable zone (no methane clathrate would have formed if the pore waters were not already saturated) but containing no dissolved methane outside the stable zone. Upon destabilization of a thin layer on a given time step, the methane so released is distributed throughout the layer in which the release occurs, corresponding to infinite diffusion within a given model layer. Destabilized methane is assumed to form methane bubbles which are advected upward with velocity w of 10^{-6} m s^{-1}.

As the ocean columns warm in response to a surface temperature perturbation, some methane can be destabilized at the bottom of the stability zone while methane clathrate above remains stable. In any given simulation we allow destabilized methane below a stable layer to do one of two things: In the no fracture case, we assume that the methane is advected into the stable zone with advection velocity $w(1-f)$, where f is the local pore fraction filled with clathrate. All of the methane which enters the stable zone is assumed to refreeze at the end of each 60-day time step. We use upstream differencing to solve the advection equation, which introduces numerical diffusion with a diffusion coefficient less than 10^{-5} m^{-2} s^{-1}, so that nonnegligible methane amounts enter the first 2-3 layers within the stability zone. In the fracture case, we set $w=0$ at and above the base of the stable zone and compute the volume expansion tendency for the destabilized layers. Whenever the volume expansion tendency exceeds a fraction γ of the overlying sediment volume, we assume that fracturing occurs which releases the excess pressure. For our base case we use γ=0.1, but we also present sensitivity tests showing the effect of alternative thresholds for fracture release.

Atmospheric Methane Model

Atmospheric methane concentration C_{CH4} is determined from a one box model represented by the equation,

$$\frac{dC_{CH4}}{dt} = f_n + f_a + f_c - \frac{C_{CH4}}{\tau} \qquad (4)$$

where f_n is the flux of methane from natural sources required to give the preindustrial atmospheric methane inventory of 1.7 Gt C (corresponding to a concentration of 0.65 parts per million by volume (ppmv)) for the initial atmospheric methane residence time τ_o; f_a is the direct flux due to anthropogenic activities, such as fossil fuel use and agriculture; f_c is the flux due to methane clathrate destabilization; and τ is a time-dependent methane atmospheric residence time. In the first set of experiments, only methane release due to clathrate destabilization and natural fluxes are con-

sidered, while for the coupled climate-carbon cycle-clathrate model, various scenarios for f_n (along with anthropogenic CO_2 emissions) are assumed.

As a result of CH_4-OH interaction, an increase in CH_4 concentration will increase the residence time, thereby further increasing the CH_4 concentration and acting as a positive feedback. This feedback is highly dependent on tropospheric NO_x concentration. *Osborn and Wigley* [1992] proposes the following theoretical relationship between atmospheric methane concentration and residence time,

$$\tau = \tau_0 \left(\frac{C}{C_0}\right)^{0.238} \tag{5}$$

which is adopted here except when indicated otherwise.

Another potentially important feedback is a possible increase in the natural methane flux f_n as climate warms. This flux is primarily from wetlands, ranging from tropical to polar latitudes. Higher temperatures could increase CH_4 emissions from wetlands both by enhancing metabolic rates [*Whalen and Reeburgh*, 1990] and by enhancing primary productivity [*Whiting and Chanton*, 1993], but a drop in the water table could lead to decreases in CH_4 production. Except where indicated otherwise, we assume f_n to be constant. For sensitivity experiments with f_n-climate feedback, we allow f_n to vary using a Q_{10} formulation, whereby

$$f_n=(f_n)_0(Q_{10})^{\frac{\Delta T_a}{10}} \tag{6}$$

where $(f_n)_0$ is the initial value of f_n and ΔT_a is the atmospheric warming.

We assume that all of the methane removed from the atmosphere is done so by oxidation to CO_2, although in reality a few percent is believed to be removed by soils. The CO_2 source due to CH_4 oxidation, f_{CO2}, is given by

$$f_{CO2} = f_{CH4} - \frac{dC_{CH4}}{dt} \tag{7}$$

where f_{CH4} is the total methane flux to the atmosphere.

Oceanic Uptake of CO_2

The oceanic uptake of CO_2 is modeled using the convolution integral of *Maier-Reimer and Hasselmann* [1987]; that is, the perturbation $\Delta C(t)$ of atmospheric CO_2 concentration due to an emission scenario $f(t)$ beginning at time t=0 is given by

$$\Delta C(t) = \int_0^t f(t')G(t-t')dt' \tag{8}$$

where $G(t)$ is the impulse response, which can be conveniently represented as

$$G(t)=A_0+\sum A_i e^{-t/\tau_i} \tag{9}$$

In the first set of experiments, $f(t)$ is given by the source due to methane oxidation alone, while for the coupled climate-carbon cycle-clathrate model, fluxes due to anthropogenic fossil fuel emissions are included.

The impulse response $G(t)$ was derived by *Maier-Reimer and Hasselmann* [1987] from simulations of CO_2 uptake by their three-dimensional ocean general circulation model. They derived three different values of $G(t)$, corresponding to successively larger cumulative CO_2 emissions into the atmosphere, and we allow for a continuous change in $G(t)$ as cumulative emissions increase. Use of $G(t)$ in the convolution integral (8) accurately represents the response of the ocean GCM but at negligible computational cost. The impulse response $G(t)$ does not include the effect of dissolution of carbonate sediments on the ocean's ability to absorb atmospheric CO_2, as this process is not included in the ocean GCM from which $G(t)$ was derived. This is a 10^3 yr and longer timescale process, so its neglect will have very little influence on the peak atmospheric CO_2 concentrations obtained here but causes atmospheric CO_2 to decrease too slowly as total emissions decrease.

Biosphere Model

For experiments using the coupled climate-clathrate model we include the six-box terrestrial biosphere model of *Harvey* [1989b]. This allows us to include an additional CO_2 sink due to stimulation of photosynthesis by higher atmospheric CO_2 concentration and warmer temperatures, as well as additional sources due to a temperature-induced increase in respiration and due to land use changes. In all experiments we use a CO_2 stimulation factor β of 0.48 and Q_{10} values for respiration of 2.0. To avoid a spurious source of carbon to the atmosphere in the coupled runs, we reduce the computed respiration flux from the biosphere to the atmosphere by the natural methane flux of carbon, f_n.

Climate Model

The one-dimensional, globally averaged atmosphere-ocean model of *Harvey and Schneider* [1985] is used to compute time-dependent temperature changes at the surface and as function of depth in the ocean. An advantage of using simple models such as used here is that the climate model sensitivity to a given heating perturbation can be readily altered to replicate that obtained by more complex models, as explained by *Harvey and Schneider* [1985]. Two versions of the ocean model are used, a pure diffusion (PD) version and an upwelling-diffusion (UD) version. The surface transient temperature response is slower in the PD version than in the UD version and the steady state warming in the ocean is uniform with depth and equal to the surface warming. In the UD version the steady state ocean temperature perturbation decreases with depth z as $e^{-z/H}$, where $H \sim 400$-500 m, if the temperature of bottom water formation in polar regions is constant [see *Harvey and Schneider*, 1985]. On the other hand, the UD model gives a vertically uniform deep ocean warming if the temperature of bottom water formation is assumed to warm by the same amount as the mean mixed layer warming. A decrease in the strength of upwelling as surface temperature increases can result in substantially greater ocean warming in the mid thermocline (300 to 600-m depth) than at the surface, as shown by *Harvey and Schneider* [1985].

In coupling the marine clathrate release model to the climate model, the temperature changes in the one-dimensional ocean model for the depths corresponding to the depths of the sediment-water interface of each sediment column are used as an upper boundary condition. Since the release of methane depends critically on whether or not $(\Delta T_{cr})_0$ is exceeded, the methane release from marine columns could, in principle, depend significantly on whether the PD or UD model version is used, and whether the temperature of bottom water formation and upwelling velocity are assumed to change in the UD version.

The columns representing high-latitude permafrost regions are driven at their upper boundaries by a thermal perturbation equal to twice the atmospheric perturbation of the globally averaged model, reflecting the greater warming projected at high latitudes than in the global average.

The climate model itself is driven by the globally averaged heating perturbation at the tropopause due to the CH_4 and CO_2 increases. These perturbations are given by

$$Q = 0.0398(\sqrt{C} - \sqrt{C_0}) \quad \textit{for } CH_4 \tag{10}$$

$$Q = 4.2(\ln(C/C_0))/\ln 2 \quad \textit{for } CO_2 \tag{11}$$

where C is the concentration of CH_4 (parts per billion by volume (ppbv)) or CO_2 (ppmv) and C_o is the initial concentration. In the first part of our study, in which we investigate the response characteristic of the marine and terrestrial clathrate columns without coupling to the climate model, we compute radiative forcings using $C_o = 350$ ppmv for CO_2 and 1700 ppbv for CH_4 (corresponding roughly to present-day conditions), while in the coupled clathrate-climate model simulations, which begin in 1760, we use $C_o = 280$ ppmv for CO_2 and 650 ppbv for CH_4.

Results

We first present the separate responses of the terrestrial columns and marine columns to a series of step function surface temperature increases. This is followed by results from the coupled climate-clathrate model.

Methane Release From Terrestrial Permafrost Regions

It is generally expected that the land surface warming at high latitudes associated with greenhouse gas increases will be 2 to 3 times the globally averaged surface air warming [see, for example, *Mitchell et al.*, 1990]. We therefore consider the impact of three step-function surface temperature perturbations: 5°C, 10°C, and 15°C, which could be associated with a globally averaged warming of 2.5°C to 5°C. Warming of this magnitude could occur by the end of the 21st century or sooner [*Harvey*, 1989a; *Bretherton et* al., 1990].

Figure 4 shows the cumulative CH_4 release to the atmosphere during the first 5000 years for all three perturbations, using the base case methane amount (5% of pore space). Because we assume that no terrestrial clathrate will be released to the atmosphere until the mean annual temperature reaches -1°C at all points above the initial clathrate zone, and this condition is satisfied for only one column with a 5°C surface warming, comparatively little methane is released using a 5°C perturbation. Furthermore, since the only column susceptible to release of its methane in this case has a thin initial clathrate zone (see Table 5), the total release occurs comparatively quickly. Nevertheless, no release occurs at all during the first 370 years after the step function surface warming, as this is the time required for the temperature threshold to be satisfied and the upper part of the stable zone to begin destabilization. Complete release of the destabilized methane occurs during the subsequent 2300 years, with a spike in the rate of release at the end of this time period. The spike is due to the merging of destabilized zones which had grown inward from the top and bottom of the initial stability zone. The merger occurred after the permafrost at the top of the column had thawed, so that relatively rapid release to the atmosphere was possible.

With a 10°C surface warming, six columns, containing 327 Gt C, will eventually release all of their methane. Hence

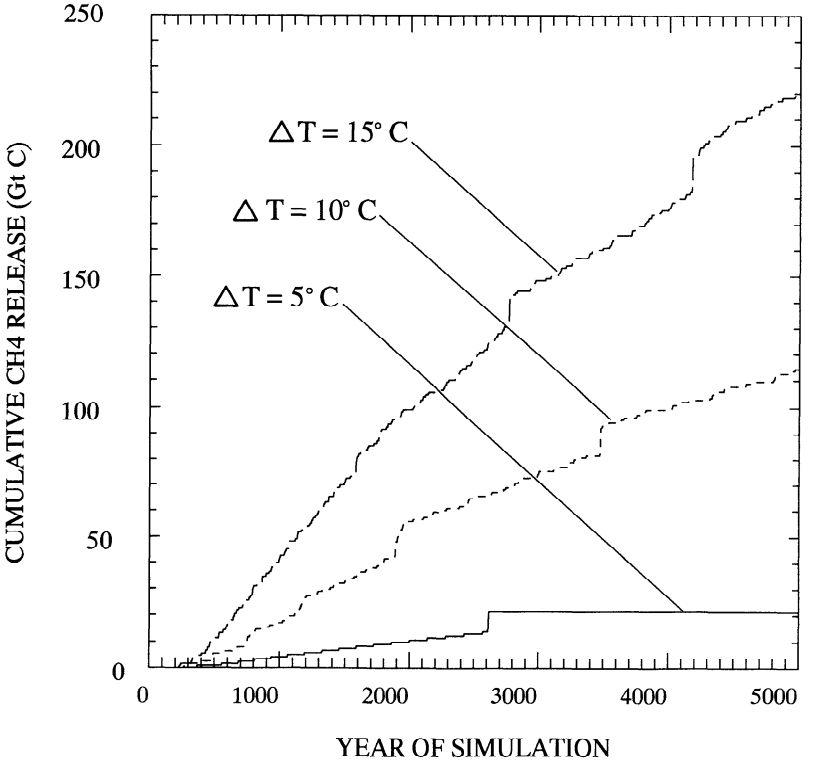

Figure 4. Cumulative release of methane (Gt C) to the atmosphere from land columns following step-function surface temperature perturbations of 5°C, 10°C, and 15°C.

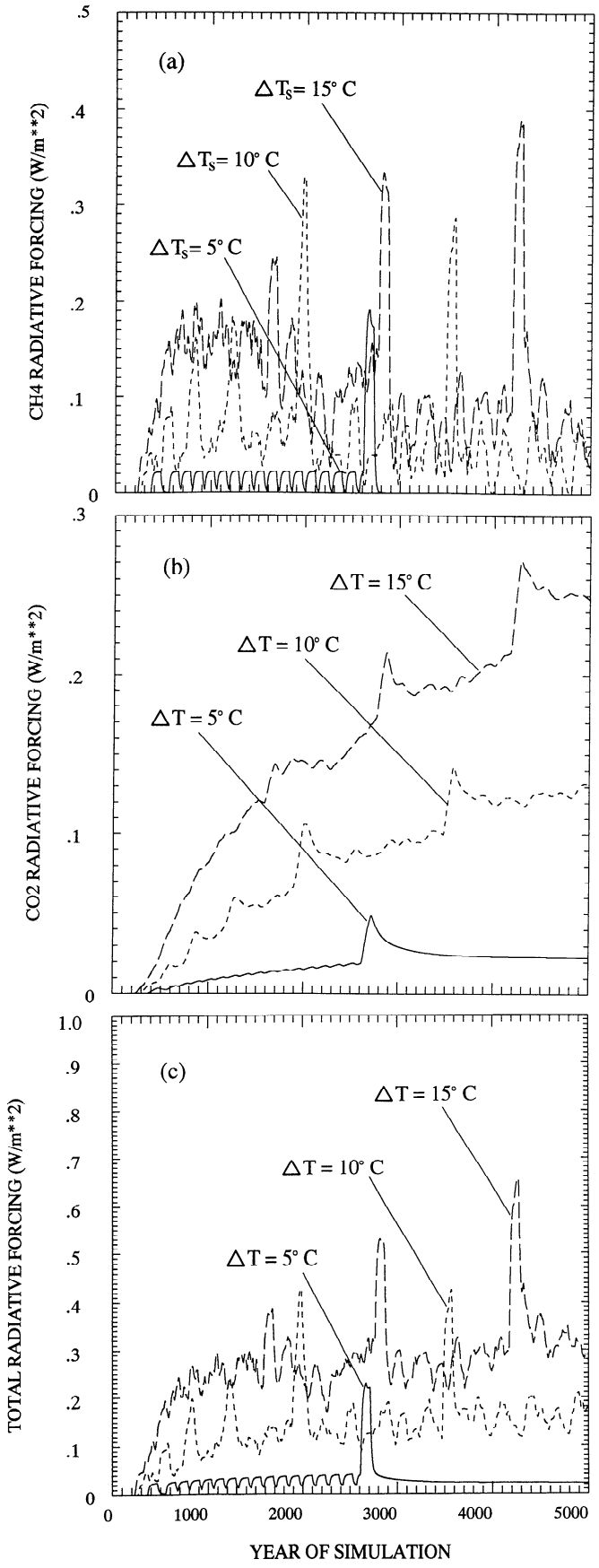

Figure 5. 100-year running mean radiative forcing (W m^{-2}) due to (a) CH_4 alone, (b) CO_2 alone, and (c) CH_4+CO_2 resulting from methane release from land columns following step-function surface temperature perturbations of 5°C, 10°C, and 15°C.

Table 6. Impact of a Step Function Surface Temperature Warming on Cumulative Methane Release From Land Columns (Gt C) and Peak Radiative Forcing (W m^{-2}) Averaged Over 100 Years for the Base Case

	Surface Warming		
	5°C	10°C	15°C
Time, years	*Cumulative Release, Gt C*		
100	0.0	0.0	0.0
500	0.8	5.5	10.8
1000	4.1	17.0	41.9
2000	10.5	55.9	99.1
5000	21.4	114.0	220.3
	Peak Forcing, W m^{-2}		
CH_4 only	0.19	0.33	0.39
CH_4 + product CO_2	0.23	0.43	0.65

the response to surface warming is highly nonlinear, with no release for perturbations of up to 4°C in our simulations. Furthermore, the response timescale increases with increasing surface perturbation, as columns with colder surface temperatures but thicker clathrate stability zones participate.

Figure 5 shows the 100-year running mean radiative forcing due to CH_4, CO_2, and CH_4+CO_2, while Table 6 summarizes the cumulative release and peak radiative forcing. During the first 2-3000 years the radiative heating due to CH_4 is greater than that due to CO_2, but thereafter the CO_2 radiative heating is larger. The total heating during most of the simulation is 0.02-0.04 W m^{-2} for a 5°C perturbation, 0.1-0.2 W m^{-2} for a 10°C perturbation, and 0.2-0.3 W m^{-2} for a 15°C perturbation, although much larger spikes occur sporadically.

Methane Release From Oceanic Sediments

In this section we examine the impact on marine clathrate of step-function temperature increases of 1°C to 6°C applied at the sediment-water interface. The base case assumes that clathrate fills 5% of the pore space at the top of the stable zone and 20% at its base. We first examine the impact on cumulative methane release of allowing fracturing in response to pressure buildup below the stable zone, or allowing upward migration of destabilized methane into the stable zone (henceforth referred to as the no-fracture case). Table 7 compares the cumulative release at selected times for the fracture case with γ=0, 0.01, 0.1, and ∞, and for the no-fracture case. When γ=0, any pressure increase that would occur due to volumetric expansion of destabilized methane leads to an immediate release of excess methane, while for γ=∞, excess methane is never released until the column is completely destabilized. Initially, there is almost no difference between the cases, as expected, but after 2000 years about twice as much methane has been released when γ=0 compared to γ=∞. The fracture case with γ=0.1 is similar to the no-fracture case, giving a modestly greater release than

Table 7. Comparison of Cumulative Methane Release to the Atmosphere (Gt C) From Ocean Columns Following a 3°C Step Function Temperature Increase

Time, years	Fracture Case γ=0	γ=0.01	γ=0.1	γ=∞	Nonfracture Case
100	84	79	77	77	83
500	261	218	180	178	191
1000	390	322	241	215	233
2000	552	468	306	251	275

Results are given for cases in which fracturing is allowed with γ = 0, 0.01, 0.1, and ∞, and for the case in which upward migration of destabilized methane into the stable zone is permitted (nonfracture case).

the case with γ=∞. In all subsequent experiments we use the fracture case with γ=0.1.

Table 8 gives the cumulative methane release after selected time intervals the peak 100-year running mean methane flux and radiative forcing due to CH_4 alone, CO_2 alone, and CH_4+CO_2 for step function temperature perturbations at the sediment-water interface of 1°C to 6°C. Also given in Table 8 for cases of 3°C and 6°C perturbations are results when the methane concentration-atmospheric residence time feedback is suppressed. Figure 6 shows the radiative forcings for a 3°C temperature perturbation with the usual methane residence time feedback.

As the temperature forcing increases from 1°C to 6°C, the cumulative methane release after the first 100 years

Table 8. Impact of a Step Function Temperature Increase at the Sediment-Water Interface on Cumulative Methane Release (Gt C) from Marine Columns and on 100-year Running Mean Peak Methane Flux (Gt C yr^{-1}) and Radiative Forcing (W m^{-2})

Case Warming	Base 1°C	Base 2°C	Base A 3°C	Base 3°C	Base 4°C	Base 5°C	Base A 6°C	6°C
				Cumulative CH_4 Release, Gt C				
100 years	7	12	77	77	83	119	160	160
200 years	13	17	116	116	123	180	241	241
500 years	27	28	180	180	192	284	402	402
1000 years	38	44	240	240	254	407	583	583
2000 years	52	71	306	306	368	586	765	765
				Peak CH_4 Flux, Gt C yr^{-1}				
	0.10	0.31	1.06	1.06	1.73	2.43	3.27	3.27
				Peak Radiative Forcing, W m^{-2}				
CH_4	0.19	0.41	1.53	1.15	1.97	2.64	3.39	2.49
CO_2	0.07	0.10	0.28	0.28	0.45	0.70	0.87	0.87
CH_4 + CO_2	0.22	0.42	1.67	1.25	2.16	2.94	3.78	2.75

Base case: The base case clathrate distribution is adopted and a fracture flux with γ=0.1 and atmospheric CH_4 residence time feedback are included. A: Same as base case except no atmospheric CH_4 residence time feedback occurs.

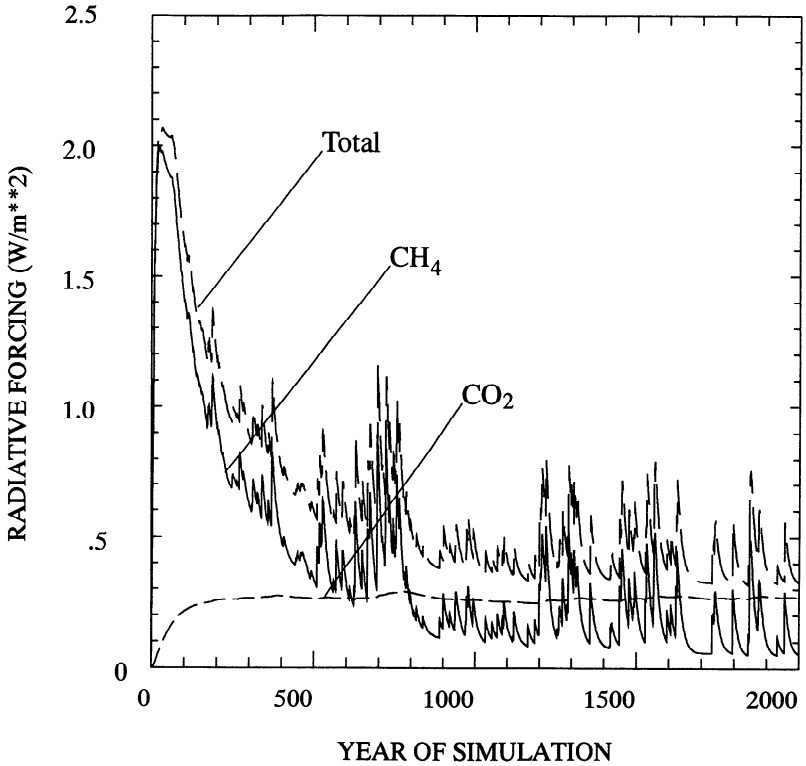

Figure 6. Radiative forcing (W m^{-2}) due to CH_4 alone, CO_2 alone, and CH_4+CO_2 resulting from methane release from oceanic columns for the base case clathrate distribution with 3°C warming at the sediment-water interface.

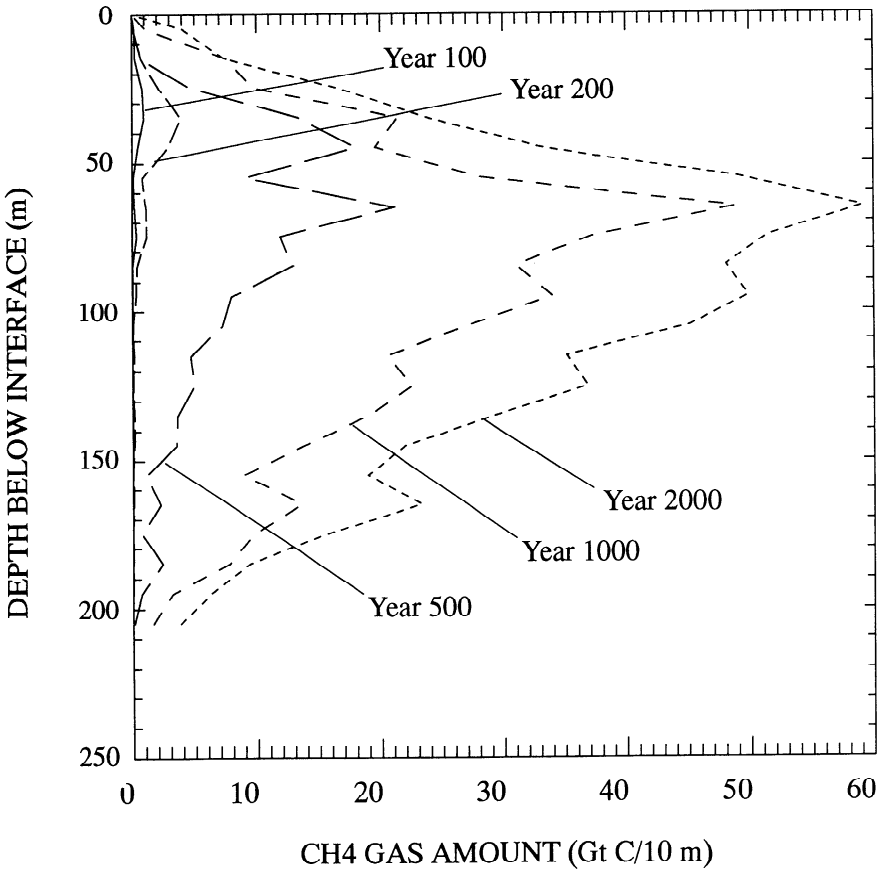

Figure 7. Variation with depth in the cumulative methane release to the atmosphere from oceanic sediments 200, 500, 1000, and 2000 years after applying a step function 3°C warming at the sediment-water interface.

increases from 7 to 160 Gt C, while the peak CH_4+CO_2 radiative forcing increases from 0.29 to 3.79 W m^{-2}. Relative to the case without atmospheric residence time feedback, inclusion of the residence time feedback (as in the base cases) enhances the peak 100-year mean CH_4 radiative forcing by 33% for a 3°C temperature forcing and by 36% for a 6°C temperature forcing. However, because of the long lifespan of CO_2 relative to that of CH_4, inclusion of this feedback has very little effect on the forcing due to the CO_2 produced by oxidation of CH_4 (see Table 8).

Figure 7 shows the distribution of the released CH_4 in terms of its initial depth below the sediment-water interface for ΔT = 3°C. Even after 2000 years, the bulk of the released CH_4 is from the top 200 m of sediment (this is true for all the temperature perturbations considered here). Thus to obtain a better estimate of the amount of methane-clathrate susceptible to destabilization as climate warms, data from the top 200 m of ocean sediments will be adequate. Furthermore, since the thickness of Quaternary sediments on continental slopes is usually at least 200 m, most of the released CH_4 in our simulation comes from Quaternary or late Tertiary sediments, so that temperatures at the sediment-water interface at the time of organic matter accumulation would have been similar to those at present. Thus any methane produced soon after sediment accumulation would have been able to form clathrate rather than escaping from the sediment column.

Coupled Climate-Carbon Cycle-Clathrate Model

In our third set of experiments, we couple the terrestrial and marine clathrate models to the climate-carbon cycle model of *Harvey* [1989a]. The climate-carbon cycle model is driven by scenarios of anthropogenic CO_2, CH_4, and CFC emissions as well as by specified N_2O concentrations. The simulation begins in 1760, at which point both the climate and the carbon cycle are assumed to have been in steady state. Three fossil fuel CO_2 emission scenarios are considered: a low scenario, in which emissions are held constant at the 1990 level until 2000, then decrease by 1% per year; an intermediate scenario, in which emissions increase by 1.0% per year until 2050, followed by a 1% per year decrease; and a high scenario, in which emissions increase by 1.5% per year until 2100, followed by a 1% per year decrease. In all cases, CFC emissions are reduced to zero by 2000 (and replacements are assumed to have no heating effect), and N_2O concentration increases from a preindustrial value of 0.280 ppmv to 0.303 ppmv in 1980 and 0.327 ppmv in 2000, after which it is held constant in concentration.

With regard to CH_4, we assume a fixed natural CH_4 flux of 0.148 Gt C yr^{-1} and a preindustrial atmospheric residence time of 10 years. The anthropogenic flux is assumed to increase from zero in 1760 to 0.14 Gt yr^{-1} and 0.20 Gt C yr^{-1} for the cases with and without residence time feedback, respectively. These assumptions result in preindustrial and

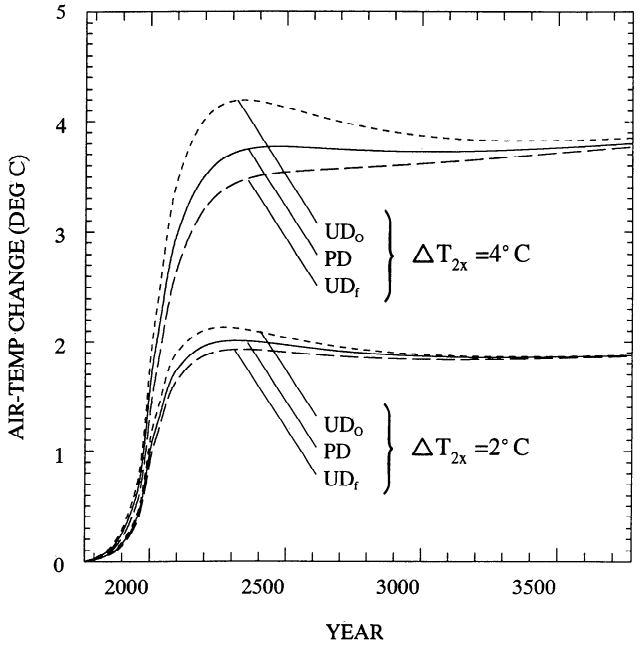

Figure 8. Transient globally averaged surface air temperature response for the medium emission scenario, low and high climate sensitivity, and the three ocean model versions without methane clathrate.

1990 atmospheric CH_4 concentrations of 0.70 and 1.61 ppmv, respectively, in rough accord with observations. We assume that anthropogenic emissions increase to 0.20 Gt C yr^{-1} (with residence time feedback) or 0.28 Gt C yr^{-1} (without residence time feedback) by 2050, then decrease to the 1980 level by 2100.

The greenhouse gas increases, whether directly specified (N_2O) or computed from specified emissions (CO_2, CH_4, and CFCs), serve to drive a globally averaged atmosphere-ocean model. As noted above, a surface perturbation equal to 2 times the globally averaged surface air temperature change is used to drive the terrestrial clathrate columns, while the depth-dependent temperature change computed by the ocean model is used to drive the marine clathrate columns. To explore a wide range of possible climate-clathrate feedback strengths, we consider three ocean model formulations: (1) a purely diffusive (PD) version; (2) an upwelling-diffusion version with fixed upwelling velocity (UD_0); and (3) an upwelling-diffusion version with upwelling velocity decreasing by 10% for each 1°C surface warming (UD_f). The temperature-upwelling velocity feedback used here in the UD_f version is consistent with that obtained by *Harvey* [1994] in a dynamical, two-dimensional ocean model during the first few hundred years of the transient response. Finally, we consider low and high climate model sensitivities, where the steady state surface air temperature warming for a carbon dioxide doubling (ΔT_{2x}) is 2°C and 4°C, respectively.

Figure 8 compares the transient response for the medium emission scenario, low and high climate sensitivity, for the three ocean versions without methane clathrate. The slowest transient response occurs for the UD_f ocean model because a large net heat flux into the deep ocean occurs as the thermohaline circulation, which provides an upward heat flux to the mixed layer, weakens [see *Harvey and Schneider*, 1985]. The fastest transient occurs for the UD_0 ocean model. However, the difference in transient response between the three ocean models is small compared to the impact of a factor of 2 uncertainty in climate sensitivity.

Table 9 gives the globally averaged surface air temperature increase at selected times during the first 2000 years of the simulation for all three emission scenarios, high and low climatic sensitivity, and the PD ocean model without and

Table 9. Globally averaged surface air temperature increase (°C) for low, medium, and high emissions scenarios, low and high climate sensitivity, and the pure diffusion ocean model

Emission Scenario	Low		Medium		High	
Climate Sensitivity	Low	High	Low	High	Low	High
Year			*No CH_4-Clathrate*			
2000	0.88	1.31	0.89	1.32	0.90	1.33
2100	1.15	1.92	1.65	2.68	2.26	3.54
2500	1.18	2.22	1.91	3.54	3.63	6.68
3000	1.20	2.37	1.84	3.62	3.36	6.59
3770	1.29	2.59	1.87	3.77	3.24	6.54
			With CH_4-Clathrate			
2000	0.89	1.35	0.90	1.36	0.90	1.36
2100	1.20	2.17	1.74	3.01	2.38	3.96
2500	1.27	2.65	2.08	4.24	3.97	8.18
3000	1.27	2.84	1.96	4.23	3.62	8.73
3770	1.36	3.01	1.96	4.50	3.44	8.60
			Difference			
2000	0.01	0.04	0.01	0.04	0.00	0.03
2100	0.05	0.25	0.09	0.33	0.12	0.42
2500	0.09	0.43	0.17	0.70	0.34	1.50
3000	0.07	0.47	0.12	0.61	0.26	2.14
3770	0.07	0.42	0.09	0.73	0.20	2.06
			Cumulative Release From Permafrost			
2000	0.0	0.0	0.0	0.0	0.0	0.0
2500	0.0	0.0	0.0	0.8	0.8	3.9
3000	0.0	3.3	0.0	8.8	6.5	29.0
3770	0.0	8.2	0.0	20.7	14.6	78.2
			Cumulative Release From Marine Sediments			
2000	0.3	1.0	0.3	1.0	0.3	1.0
2500	23.9	65.9	46.1	115.0	106.0	230.0
3000	37.6	117.0	72.2	184.0	168.0	510.0
3770	53.4	171.0	101.0	256.0	210.0	809.0
			Fraction of Marine Release Due to Fracturing			
3770	0.43	0.34	0.46	0.20	0.18	0.06

Also given are the cumulative methane release (Gt C) from marine and terrestrial columns, as well as the fraction of total release from marine columns due to parameterized fracturing.

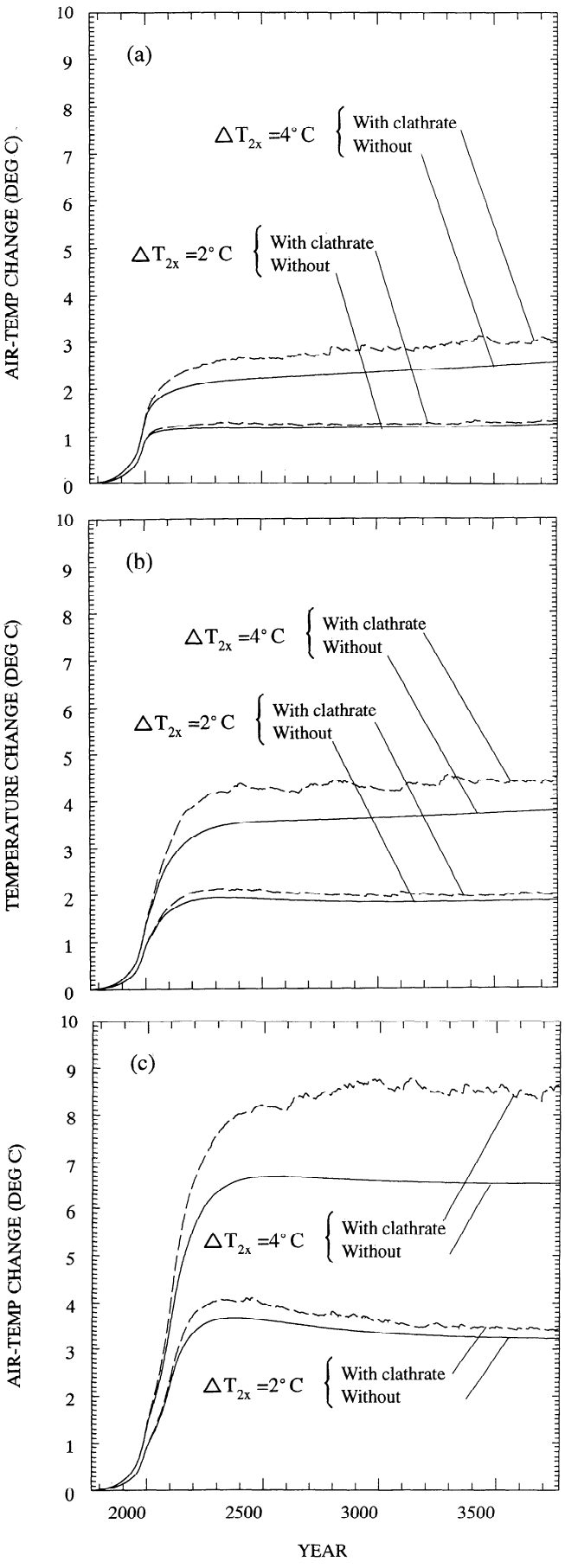

with methane clathrate. For the cases with clathrate the base case clathrate amounts are assumed (20% of pore space filled with clathrate at the base of the stable zone in each column, decreasing to 5% at the top). Also given are the differences in warming between the cases with and without clathrate, the cumulative methane release from permafrost and marine columns for the cases with clathrate, and the fraction of total marine clathrate release due to parameterized fracturing. Figure 9 compares the transient surface air temperature responses with and without methane clathrate for the PD model version for all three emission scenarios and for low and high climate sensitivity.

The key results of these simulations are as follows: (1) inclusion of methane clathrates has a small effect during the 21st century; (2) the overwhelming majority of the released methane comes from marine columns; (3) the parameterized fracture release is relatively important for the low emission, low climate sensitivity case, in which the absolute release is small but constitutes less than 10% of the total release for the high emission, high sensitivity case; (4) a doubling of climate sensitivity multiplies the absolute effect of including methane clathrate by a factor of 3-5, such that the relative enhancement of global warming due to clathrate destabilization increases as overall climatic sensitivity increases; and (5) inclusion of methane clathrate enhances the eventual climatic response to anthropogenic greenhouse gas emissions by up to about 10% for low climate sensitivity and by up to 25% for high climate sensitivity.

The relatively greater importance of the parameterized fracture release when the absolute release is small is a result of the fact that in such cases, clathrate destabilization involves columns with small $(\Delta T_{cr})_0$. These columns tend to have thin clathrate stability zones, so that any basal destabilization occurs at relatively shallow depths, where the volume expansion tendency is larger, thereby facilitating eventual sediment fracturing. With greater climate warming, clathrate destabilization increasingly occurs in columns with thicker stability zones, so that fracturing is less likely to occur. This relationship is independent of the specific criterion for fracturing which we have used. Thus to the extent that fracture-based release of destabilized methane would occur in reality, we believe that it will be less important the greater the overall climatic warming. For the case in which we allow destabilized methane to migrate into the overlying stable zone and refreeze as clathrate, the difference in warming from what is shown in Table 9 amounts to 1-2%, except for the high emission, high climate sensitivity scenario. In this case, the transient warming is up to 5% greater since some of the methane which cannot be released through fracturing can accelerate decomposition of the entire column and eventually reach the sediment-water interface.

Figure 9. Transient globally averaged surface air temperature response with and without methane clathrate columns for the pure diffusion ocean model, for low and high climate sensitivity, and for (a) the low emission scenario, (b) the medium emission scenario, and (c) the high emission scenario. Solid lines, no clathrate; dashed lines, with clathrate.

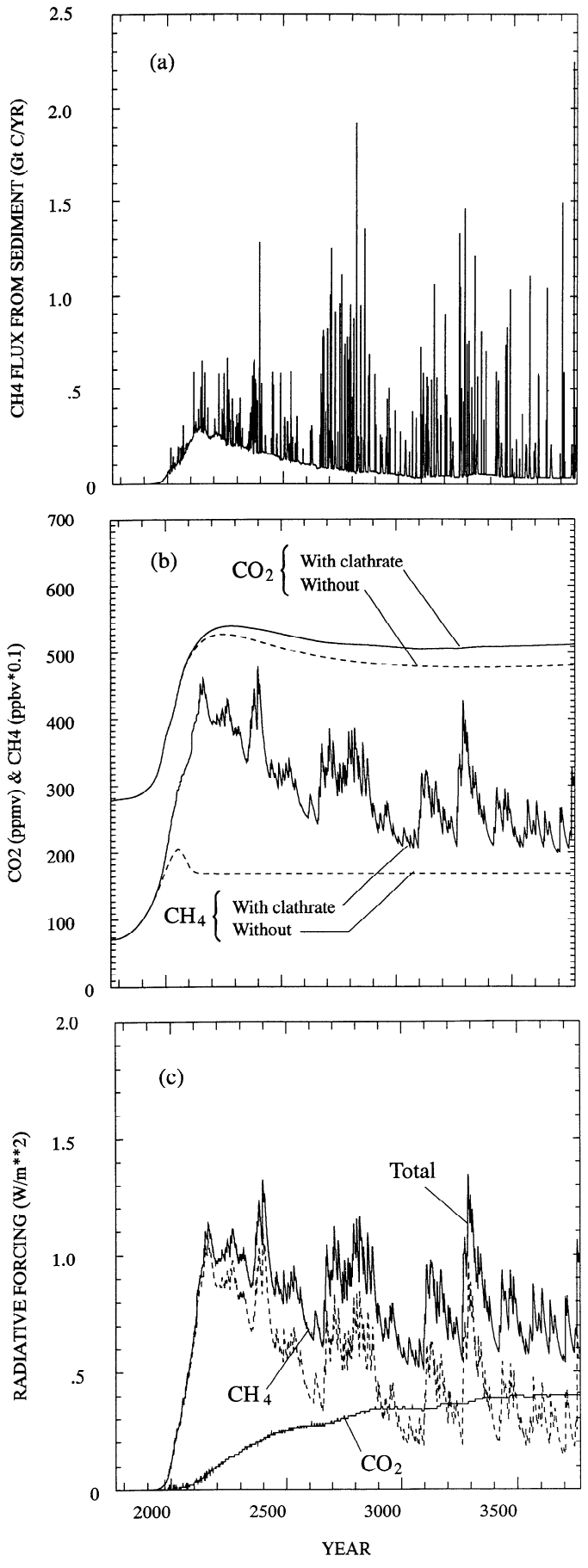

Figure 10 presents the following results for the medium emission, high sensitivity scenario using the PD ocean model: the CH_4 flux to the atmosphere from marine and terrestrial columns, the increase in atmospheric CH_4 and CO_2 concentrations due to clathrate destabilization, and the extra radiative forcing for the case with clathrate destabilization due to CH_4, CO_2, and CH_4+CO_2. The flux from oceanic sediments is highly erratic, as the threshold for sudden release of destabilized methane from individual columns occurs sporadically; yearly fluxes after 2100 of 0.5-1.5 Gt C occur several times per century, with a century-mean flux peaking around 0.3 Gt C yr^{-1}. This is somewhat less than the mean flux of 0.48 Gt C yr^{-1} estimated by *Revelle* [1983] to occur after a CO_2 doubling. The cumulative flux from our terrestrial columns is about 10% of the flux from marine columns. The combined terrestrial and marine fluxes cause the atmospheric CH_4 loading to be a maximum of 2 1/2 ppmv or about 5 Gt C greater than without clathrate destabilization and the maximum CO_2 loading to be 35 ppmv or 70 Gt C greater (Figure 10b). The extra CO_2 causes up to 0.4 W m^{-2} radiative heating and the extra CH_4 causes up to 1.0 W m^{-2} radiative heating, with the total extra radiative heating peaking at about 1.3 W m^{-2} (Figure 10c).

Table 10 illustrates the effect of using different ocean models for the medium emission, high climate sensitivity scenario. Shown in Table 10 are the globally averaged surface temperature changes without clathrate, with clathrate, the difference between clathrate and nonclathrate cases, and the cumulative methane release from permafrost and marine columns. As seen from Table 10, the methane release from marine columns is largest for the UD_f ocean model, as expected, but is not significantly different from the PD model. Use of the UD_0 ocean model reduces the maximum temperature impact of clathrate destabilization by about 25% compared to the PD ocean model and by about 35% compared to the UD_f model, since the UD_0 model produces a steady state ocean temperature perturbation which decreases with increasing depth. However, the absolute peak temperature increase is largest with the UD_0 model because of the shorter surface temperature response timescale for the UD_0 model. Differences in methane release from the terrestrial columns are very small and are related to differences in the transient surface temperature response.

In the next set of experiments we examine the importance of model nonlinearities by halving and doubling the amount of methane clathrate for the medium emission scenario, PD ocean model version, with high climate sensitivity. We consider two doubled cases: one in which the pore fraction filled with clathrate is doubled and one in which the pore fraction filled with clathrate is held at the base case value,

Figure 10. Results for the medium emission scenario with high climatic sensitivity and the pure diffusion ocean model: (a) CH_4 flux from ocean columns; (b) extra CO_2 and CH_4 atmospheric concentration (ppmv for CO_2, 100 x ppmv for CH_4) due to methane clathrate destabilization; and (c) extra CH_4, CO_2, CH_4+CO_2 radiative forcing due to methane clathrate destabilization. In Figuew 10b, solid lines are for simulations without clathrate, dashed lines with clathrate.

Table 10. Effect of Ocean Model on the Increase in Surface Temperature Response due to the Inclusion of Methane Clathrate for the Medium Emission Scenario and High Climate Sensitivity

Year	Ocean Model UD_o	UD_f	PD
	Without CH_4-Clathrate		
2000	1.78	1.56	1.32
2500	4.12	3.77	3.54
3000	3.87	3.72	3.62
3770	3.85	3.80	3.77
	With CH_4-Clathrate		
2000	1.82	1.59	1.36
2500	4.65	4.58	4.24
3000	4.25	4.43	4.23
3770	4.15	4.60	4.50
	Difference		
2000	0.04	0.03	0.04
2500	0.53	0.81	0.70
3000	0.38	0.71	0.61
3770	0.30	0.80	0.73
	Cumulative Methane Release From Permafrost		
2000	0.0	0.0	0.0
2500	2.4	2.4	0.8
3000	10.3	9.6	8.8
3770	21.4	25.0	20.7
	Cumulative Methane Release From Marine Sediments		
2000	0.7	0.8	1.0
2500	72.4	119.0	115.0
3000	99.0	198.0	184.0
3770	128.0	294.0	256.0

Also given is the cumulative methane release (Gt C) from marine and terrestrial columns.

but the assumed horizontal extent of clathrate is doubled. Total land plus ocean cumulative methane release and temperature changes due to clathrate release are given in Table 11. The cumulative release increases by a smaller proportion than the increase in clathrate amount as the pore fraction filled with clathrate increases, especially during the first few hundred years; this is because, as clathrate density increases, the rate of downward penetration of the warming anomaly decreases due to the clathrate heat of dissociation. This nonlinearity does not arise if clathrate amount is increased by increasing the horizontal extent of clathrate rather than the density. Instead, the cumulative methane release more than doubles when the methane amount is doubled. This is because, with an initially larger methane release, the climate warming is greater, so that more columns release CH_4 to the atmosphere. By year 2000 (3770 AD) the cumulative release when the clathrate area is doubled has increased by a factor of 4, implying a very strong nonlinearity. A second nonlinearity involves the atmospheric methane concentration-residence time feedback, which causes atmospheric concentrations to increase relatively faster than the increase in flux to the atmosphere. Thus as seen from Table 11, atmospheric methane concentration increases by a significantly larger factor than the increase in the cumulative release when the clathrate area is doubled. A third nonlinearity involves the radiative forcing, which increases with the square root of methane concentration. The net effect of all three nonlinearities is that the effect on global warming of clathrate destabilization increases very close to linearly with clathrate amount when the amount is increased by increasing the clathrate density but can increase substantially faster than linearly as the assumed areal extent increases.

The key to the nonlinear behavior when the areal extent of clathrate increases is to generate a warming large enough

Table 11. Effect of Uncertainty in the Amount of CH4-Clathrate on Global Mean Temperature Change, Cumulative Methane Release, and the Perturbation in Atmospheric CH_4 Concentration for the Medium Emission, High Climatic Sensitivity Scenario

Year	2.5-10%	5-20%	10-40%	Double area
	Global Warming With Clathrate			
2000	1.36	1.36	1.36	1.40
2100	2.95	3.01	3.10	3.40
2500	3.91	4.24	4.73	5.05
3000	4.01	4.23	4.88	5.34
3770	4.22	4.50	5.28	7.17
	Extra Warming Due to Clathrate			
2000	0.04	0.04	0.04	0.08
2100	0.27	0.33	0.42	0.72
2500	0.37	0.70	1.19	1.51
3000	0.39	0.61	1.26	1.72
3770	0.45	0.73	1.51	3.40
	Cumulative CH_4 Release (Land+Ocean Columns), Gt C			
2000	1.0	1.0	1.0	2.1
2500	67.9	115.8	184.3	269.9
3000	106.2	192.8	353.0	478.2
3770	133.1	276.7	547.4	995.4
	Perturbation in Atmospheric CH_4 Concentration, ppmv			
2000	0.22	0.22	0.22	0.47
2500	0.52	1.39	3.16	3.86
3000	0.57	0.53	2.06	3.89
3770	0.78	1.29	2.05	10.64

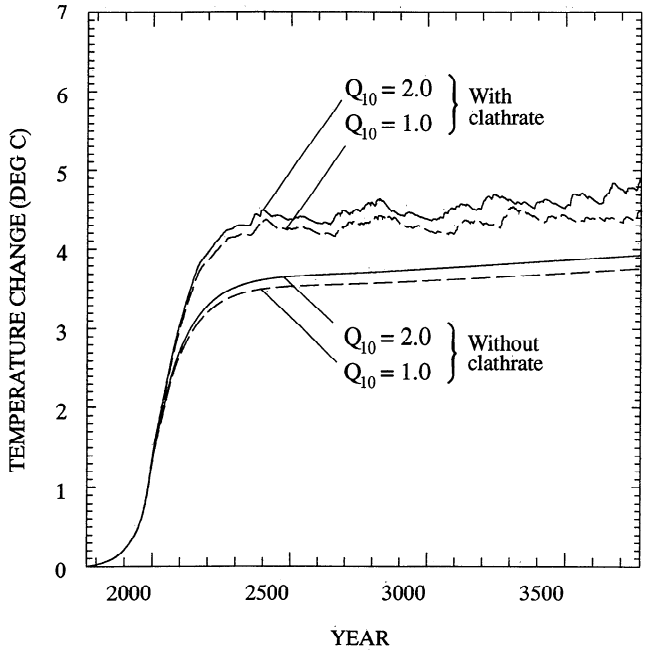

Figure 11. Global mean air temperature warming for the medium emission, high climate sensitivity scenario for cases with (Q_{10} = 2.0) and without (Q_{10} = 1.0) a climate-wetland methane flux feedback and with and without methane clathrate destabilization.

that columns with $(\Delta T_{cr})_0$ > 4°C release methane to the atmosphere, since columns with $(\Delta T_{cr})_0$ > 4°C contain significant amounts of methane in our simulations. For low emission scenarios and/or low climate sensitivity this threshold is not reached. In reality, the threshold for nonlinear behavior and the extent of the nonlinearity are likely different than obtained here. We have simply demonstrated the possibility of strongly nonlinear behavior and the circumstances under which it can occur.

In our final set of experiments we examine the effect of incorporating a feedback between the natural methane flux, f_n, and the atmospheric temperature change, using a Q_{10} value of 2.0 (see equation (6)). Figure 11 compares the atmospheric temperature response for the medium emission, high sensitivity case, for which it can be seen that the natural flux feedback enhances the peak temperature response by about 5%.

System Feedback Analysis

For a linear feedback system the steady state temperature response to a heating perturbation ΔQ is given by

$$\Delta T = \frac{G_0}{1-f}\Delta Q \qquad (12)$$

where G_0 is the system gain (equal to $\partial F/\partial T$, where F = outgoing emission to space and the derivative is evaluated at the effective planetary radiating temperature) and f, the total system feedback factor, is the linear sum of individual feedback factors f_i. Each f_i is given by $G_o\Delta J_i/\Delta T$, where ΔJ_i is the change in net radiation due to the change in internal variable i acting alone. The individual feedback factor f_i can be thought of as the intrinsic feedback strength. For a linear system the individual f_i are constant and hence independent of the magnitude of ΔQ or ΔT, but it can be readily seen from equation (12) that the effect on the steady state temperature change of adding a feedback of given intrinsic strength is larger the greater the preexisting positive feedback (i.e., the larger the preexisting value of f). *Lashof* [1989] estimated f_i for methane clathrate destabilization to be in the range 0.01-0.20.

Table 12. Clathrate Feedback Factors Computed From the Last 500 Years of Simulations With the Coupled Climate-Clathrate Model

Emission Scenario	Low		Medium		High	
Climate Sensitivity	Low	High	Low	High	Low	High
ΔT, °C	1.32	3.00	1.96	4.39	3.48	8.51
$\Delta J_{clathrate}$, W m^{-2}	0.15	0.55	0.24	0.77	0.44	2.12
$f_{clathrate}$	0.030	0.049	0.034	0.047	0.033	0.066

Although the above formalism strictly applies only to steady state temperature changes and radiative heating perturbations, the radiative forcing due to clathrate destabilization and overall temperature change are relatively constant during the last 500 years of our simulations. We compute $\Delta J_{clathrate}$ as the difference in total CO_2+CH_4 radiative heating for model runs with and without clathrate columns present. Table 12 shows the clathrate destabilization feedback factor calculated for our scenarios, along with the corresponding mean $\Delta J_{clathrate}$ and ΔT values. The computed feedback factor is consistently larger for the high sensitivity case and tends to increase with increasing anthropogenic GHG emissions, indicating that the overall feedback is nonlinear. For low climate sensitivity, $f_{clathrate}$ ranges from 0.030 to 0.033, while for high climate sensitivity it ranges from 0.047 to 0.066.

The feedback factor doubles in value in going from the high emission, low climate sensitivity case to the high emission, high sensitivity case. Examination of the distribution of cumulative methane release by column $(\Delta T_{cr})_0$ category indicates that for all cases except the high emission, high sensitivity case, the overwhelming majority of the released methane comes from columns where $(\Delta T_{cr})_0$ < 4°C. For the high emission, high sensitivity case, columns where $(\Delta T_{cr})_0$ = 4-7°C are also destabilized and since, in our particular model, these columns contain substantial amounts of methane (see Table 3), there is an abrupt increase in the

Table 13. Comparison of $f_{wetland}$ and $f_{clathrate}$

	Alone	In Combination
$f_{wetland}$	0.013	0.016
$f_{clathrate}$	0.046	0.049

Results for each feedback factor are given when only one of these feedbacks is operative, and when both feedbacks are operative.

climate-clathrate feedback strength. We stress that the true distribution of clathrate with respect to $(\Delta T_{cr})_0$ is unknown. Our results merely serve to underline the value of this parameter in understanding the behavior of the coupled climate-clathrate system and to illustrate the potential for significant nonlinearities in the system behavior.

For comparison purposes we also computed the feedback factor associated with the feedback between the natural flux of methane and the climate which we obtained using a Q_{10} of 2.0. We shall designate this feedback factor as f_{wetland}, since most of the natural methane flux comes from wetlands. Table 13 gives values of f_{wetland} obtained from pairs of runs for the medium emission, high climate sensitivity case with and without methane clathrates included. Also shown are values of $f_{\text{clathrate}}$ obtained from pairs of runs with and without the wetland feedback. Both feedback factors are slightly larger in the presence of the other feedback, with f_{wetland} about 1/3 the magnitude of $f_{\text{clathrate}}$. This result is clearly dependent on the choice of Q_{10}, which we regard as highly uncertain.

Conclusions

We have attempted to constrain the possible impact on the climatic response to anthropogenic greenhouse gas emissions of destabilization of marine and terrestrial methane clathrates. Using data on ocean depth, temperature at the sediment-water interface, ocean sediment thermal conductivity, and the geothermal heat flux on a 1° x 1° global grid, we estimate the volume of the clathrate-stable region in oceanic sediments to be 1.65×10^{16} m^3. Available data indicate that clathrate concentration tends to be highest at the base of the stable zone and decreases in concentration toward the top of the stable zone, although many cases have been reported of clathrates recovered from or inferred to exist just below the sediment-water interface. Clathrates can fill as much as 50% of the pore space at the base of the stable zone, based on analysis of bottom simulating reflectors, but probably occupy a much smaller pore fraction near the top of the stable zone, based on the fact that clathrates frequently do not survive the coring process.

Because we wish to develop worst case estimates of the potential climatic impact of methane clathrate destabilization, we have adopted a number of assumptions which may tend to over-estimate the impact of clathrate destabilization. These assumptions are (1) neglect of the possible effect of lower sea level during the last ice age on present day clathrate amounts and distribution; (2) neglect of possible retention of clathrate due to incomplete decomposition; (3) neglect of possible clogging of sediment pores with methane bubbles in fine-grained sediment; and (4) neglect of possible dissolution of methane bubbles or oxidation of methane in seawater. We have also neglected possible oxidation of methane released from terrestrial clathrate before it reaches the atmosphere, but the potential error is small because the terrestrial columns contribute less than 10% of the total methane release in our simulations. Enormous uncertainties remain concerning the total amount of methane clathrate and its distribution. Despite these uncertainties we believe that we have obtained a number of useful insights into potential climate-methane clathrate feedback processes:

1. In the absence of fracturing and sediment failure, destabilized methane will not be released from a given ocean sediment column until the warming at the sediment-water interface exceeds the difference $(\Delta T_{cr})_0$ between the temperature at the interface and the destabilization temperature at the interface. Over 98% of the marine clathrate (given our simplifying assumptions) occurs in sediments where $(\Delta T_{cr})_0$ exceeds 4°C and hence is not susceptible to release until the warming at the sediment-water interface exceeds this value.

2. To the extent that fracture release of destabilized methane from below the clathrate stability zone would occur in reality, it is likely to decline in relative importance as the total global warming and cumulative methane release increase. This is because, with greater warming, columns with increasingly thick and deep clathrate stability zones become susceptible to destabilization. As a result, the volume expansion tendency accompanying clathrate destabilization is smaller and the thickness of overlying sediments is greater.

3. The relative effect of methane clathrate destabilization on global warming increases as the overall climatic sensitivity increases. This would be expected even if the intrinsic clathrate-climate feedback strength, as quantified by the feedback factor $f_{\text{clathrate}}$, were constant. However, we find that $f_{\text{clathrate}}$ itself increases with climate sensitivity and can abruptly increase with increasing anthropogenic greenhouse gas emissions. For low climate sensitivity (ΔT_{2x} = 2°C), we find that methane clathrate destabilization enhances the globally averaged surface temperature response by up to 10%, while for high climate sensitivity (ΔT_{2x} = 4°C), methane clathrate destabilization acts as a stronger feedback, enhancing the climatic response by up to 25%.

4. The climatic impact of methane clathrate destabilization increases roughly linearly with the assumed size of the methane clathrate reservoir as long as the increase in reservoir size is due to increased clathrate concentration in sediments. This is a result of nonlinearities involving the clathrate heat of dissociation, clathrate concentration-residence time feedback, and saturation of the radiative heating perturbation as CO_2 and CH_4 concentrations increase. However, the increase can be markedly faster than linear if the clathrate pool increases due to increasing horizontal extent rather than increasing clathrate concentration, for medium or high emission scenarios with high climatic sensitivity.

5. There is little difference in the climatic impact of anthropogenic greenhouse gas emissions between the different ocean model formulations (pure diffusion, upwelling diffusion with fixed temperature of bottom water formation, upwelling diffusion with upwelling velocity decreasing as mixed layer temperature increases) when our base case methane clathrate distribution is included. This near constancy is a result of the competing effects of ocean model formulation on the surface temperature transient response timescale and on the additional heating due to clathrate destabilization.

6. The circumstances under which clathrate destabilization could exert a strong positive feedback on climatic change (medium to high emission scenario and high climatic sensitivity) are also circumstances under which the projected global mean warming is large (greater than 4°C) even in the absence of clathrate destabilization, so that significant impacts on ecosystems and human societies would be expected whether or not clathrate destabilization occurs.

The most important conclusion that we draw from our analysis is that even for what are likely to be worst case

assumptions, the impact on future global warming due to inclusion of methane clathrate-climate feedback is smaller than the difference between our low, medium, and high fossil fuel CO_2 emission scenarios, or the difference between cases with low (2°C global mean steady state warming for CO_2 doubling) and high climatic sensitivity (4°C global mean steady state warming for CO_2 doubling). Uncertainty in future global warming due to potential methane clathrate destabilization is thus smaller than the uncertainty due to future fossil fuel use or climate sensitivity.

Acknowledgments. This work and Zhen Huang were supported by NSERC grant OGP0001413. We would like to thank Keith Kvenvolden, Stuart Gaffen, Bruce Buffet, and two anonymous reviewers for useful comments on the work presented here.

References

Bretherton, F.P., K. Bryan, and J.D. Woods, Time-dependent greenhouse-gas-induced climate change, in *Climate Change, The IPCC Scientific Assessment*, pp. 173-193, Cambridge University Press, New York, 1990.

Brooks, J.M., M.C. Kennicutt II, R.R. Fay, and T.J. MacDonald, Thermogenic gas hydrates in the Gulf of Mexico, *Science, 225*, 409-411, 1984.

Brooks, J.M., H.B. Cox, W. R. Bryant, M. C. Kennicutt II, R. G. Mann, and T. J. MacDonald, Association of gas hydrates and seepage in the Gulf of Mexico, *Organ. Geochem., 10*, 221-234, 1986.

Brooks, J.M., M.E. Field, and M. Kennicutt II, Observations of gas hydrates in marine sediments, offshore northern California, *Mar. Geol., 96*, 103-109, 1991.

Carl, H., and D. Harry, Ocean engineering, in *Handbook of Marine Science*, vol. 1, pp. 475-566, edited by F.G. Smith, CRC Press, Boca Raton, Fla., 1974.

Carpenter, G., Coincident sediment slump-clathrate complexes on the U.S. Atlantic continental slope, *Geo Mar. Lett., 1*, 29-32, 1981.

Chamberlin, J.W., H.M. Foley, G.J. MacDonald, and M.A. Ruderman, Climate effects of minor atmospheric constituents, in *Carbon Dioxide Review*, pp. 255-277, edited by W.C. Clark, Oxford University Press, New York, 1983.

Chanton, J.P., and C.S. Martens, Seasonal variations in ebullitive flux and carbon isotopic composition of methane in a tidal freshwater estuary, *Global Biogeochem. Cycles, 2* , 289-298, 1988.

Chen, T.S., A molecular dynamics study of the stability of small prenucleation water clusters, *Ph.D. dissertation,* University of Missouri-Rolla, Microfilms No. 8108116, Ann Arbor, Mi., 1980.

Claypool, G.E., and I.R. Kaplan, The origin and distribution of methane in marine sediments, in *Natural Gas in Marine Sediments*, pp. 99-139, edited by I.R. Kaplan, Plenum, New York, 1974.

Claypool, G.W., and K.A. Kvenvolden, Methane and other hydrocarbon gases in marine sediment, *Ann. Rev. Earth Planet. Sci., 11*, 299-327, 1983.

Davis, E.E., and R.D. Hyndman, Rates of fluid expulsion across the Northern Cascadia Accretionary Prism: Constraints from new heat flow and multichannel seismic reflection data, *J. Geophys. Res., 95*, 8869-8889, 1990.

de Roo, J.L., C.J. Peter, R.N. Lichtenthaler, and G.A.M. Diepen, *AICHE J., 29*, 651, 1983.

Devol, A.H., Methane oxidation rates in the anaerobic sediments of Saanich Inlet, *Limnol. Oceanogr., 28*, 738-742, 1983.

Dobrynin, V.M., Y.P. Korotajev, and D.V. Plyuschev, Gas hydrates: A possilbe energy resource, in *Long-term Energy Resources,* pp. 727-729, Vol. 1, Pitman, Lonton, 1981.

Freeze, R.A., *Groundwater*, 604 pp., Prentice-Hall, Inc., Englewood Cliffs, N. J., 1979.

Ginsburg, G.D., V.A. Solov'yev, R.E. Cranston, T.D. Lorenson, and K.A. Kvenvolden, Gas hydrates from the continental slope, offshore Sakhalin Island, Okhotsk Sea, *Geo Mar. Lett., 13*, 41-48, 1993.

Ginsburg, R.A., *et al.*, Gas hydrates of the southern Caspian, *Int. Geol. Rev., 34*, 765-782, 1992.

Harrison, W.E., and J.A. Curiale, Gas hydrates in sediments of holes 497 and 498A, Deep sea drilling project leg 67, in *Initial Reports of the Deep Sea Drilling Project 67*, edited by A.J. von Huene R. et al., pp. 591-594, U.S. Government Printing Office, Washington, D.C., 1982.

Harvey, L.D.D., Managing atmospheric CO_2, *Clim. Change, 15*, 343-381, 1989a.

Harvey, L.D.D., Effect of model structure on the response of terrestrial biosphere models to CO_2 and temperature increases, *Global Biogeochem. Cycles, 3*, 137-153, 1989b.

Harvey, L.D.D., Transient temperature and sea level response of a two-dimensional ocean-climate model to greenhouse gas increases, *J. Geophys. Res. 99*, 18,447-18,466, 1994.

Harvey, L.D.D., and S.H. Schneider, Transient response to external forcing changes on 10^0-10^4 year timescales, 1, Experiments with globally averaged atmosphere and ocean energy balance models, *J. Geophys. Res., 90*, 2191-2205, 1985.

Hesse, R., and W. E. Harrison, Gas hydrates (clathrates) causing pore-water freshening and oxygen isotope fractionation in deep water sedimentary sections of terrigenous continental margins, *Earth Planet. Sci. Lett., 55*, 453-562, 1981.

Hovland, M., A.G. Judd, and R.A. Burke, The global flux of methane from shallow submarine sediments, *Chemosphere, 26*, 559-578, 1993.

Hyndman, R. D., and E. E. Davis, A mechanism for the formation of methane hydrate and sea floor bottom-simulating reflectors by vertical fluid expulsion, *J. Geophys. Res., 97*, 7025-7041, 1992.

Iversen, N., and B.B. Jorgensen, Anaerobic methane oxidation rates at the sulfate-methane transition in marine sediments from Kattegat and Skagerrak (Denmark), *Limnol. Oceanogr., 30*, 944-955, 1985.

Katz, H.-R., Probable gas hydrate in continental slope east of the North Island, New Zealand, *J. Petrol. Geol., 3*, 315-324, 1981.

Kayen, R.E., The mobilization of Arctic Ocean landslides by sea level fall induced gas hydrate decomposition. *M.S. thesis*, 227 pp., Calif. State Univ., Hayward, 1988.

Kvenvolden, K.A., Methane hydrate and global climate, *Global Biogeochem. Cycles, 2*, 221-229, 1988.

Kvenvolden, K.A., and G.E. Claypool, Gas Hydrates in Oceanic Sediments, *U.S. Geol. Surv. Open File Rep. 88-216,* 50 pp., 1988.

Kvenvolden, K.A., and L.A. Barnard, Gas hydrates of the Blake Outer Ridge, site 533, deep sea drilling project leg 76, in *Initial Reports of the Deep Sea Drilling Project 76*, edited by R. E. Sheridan et al., pp. 353-365, U.S. Government Printing Office, Washington, D. C., 1983.

Kvenvolden, K.A., G.D. Ginsberg, and V.A. Solov'yev, Worldwide distribution of subaquatic gas hydrates, *Geo Mar. Lett., 13*, 32-40, 1993.

Kvenvolden, K.A., and M. Kastner, Gas hydrate of the Peruvian outer continental margin, in *Proceeding of the Ocean Drilling Program, Scientific Results, 112*, edited by E. Suess et al., pp. 517-526, Ocean Drilling Program, College Station, Tex., 1990.

Kvenvolden, K.A., and T.J. MacDonald, Gas hydrate of the Middle America Trench-Deep sea drilling project leg 84, in *Initial Reports of the Deep Sea Drilling Project 84*, edited by R. von Huene et al., pp. 667-682, U.S. Government Printing Office, Washington, D. C., 1985.

Kvenvolden, K.A., and M.A. McMenamin, *Hydrates of Natural Gas: A Review of Their Geological Occurrences*, U.S. Geol. Surv. Circ., 825, 11 pp., 1980.

Lee, W., and S. Clark, Heat flow and volcanic temperatures, in Handbook of Physical Constants, *Geol. Soc. Am. Mem. 97*, edited by S. Clark, pp. 483-511, 1966.

Lachenbruch, A., J. Sass, L. Lawver, M. Brewer, B. Marshall, R. Munroe, J. Kennelly, S. Galanis, and T. Moses, Temperature and depth of permafrost on the Alaskan Arctic Slope, in *Alaska North Slope Geology, 50*, edited by I. Tailleur and P. Weimer, Pacific Section Soc. Ec. Paliort Mineral. and Alaskan Geol. Soc., 1987.

Lachenbruch, A., J. Sass, B. Marshall, and T. Moses, Permafrost, heat flow, and the geothermal regime at Prudhoe Bay, Alaska, *J. Geophys. Res., 87*, 9301-9316, 1982.

Lashof, D.A., The dynamic greenhouse: Feedback processes that may influence future concentration of atmospheric gases and climatic change, *Clim. Change, 14*(3), 213-242, 1989.

Leggett, J., The nature of the greenhouse threat, in *Global Warming, The Greenpeace Report*, edited by J. Leggett, pp. 14-43, Oxford University Press, New York, 1990.

Louden, K.E., Marine heat flow data listing, In *Handbook of Seafloor Heat Flow*, edited by J.A. Wright and K.E. Louden, pp. 325-485, CRC Press, Boca Raton, Fla., 1989.

MacDonald, G.J., Role of methane clathrates in past and future climates, *Clim. Change, 16*, 247-281, 1990.

Maier-Reimer, E., and K. Hasselmann, Transport and storage of CO_2 in the ocean - An inorganic ocean-circulation carbon cycle model, *Clim. Dyn., 2*, 63-90, 1987.

Makogon, Y.F., *Hydrates of Natural Gas*, 237 pp., translated by W.J. Cieslewicz, PennWell, Tulsa, Ok., 1981.

Makogon, Y.F., Natural gas hydrates: The state of study in the USSR and perspectives for its use, paper presented at *the third chemical congress of North America, Toronto, Canada,* June 5-10, 1988.

Martens, C.S., and J.V. Klump, Biogeochemical cycling in an organic-rich coastal marine basin, 1, Methane sediment-water exchange processes, *Geochim. Cosmochim. Acta, 44*, 471-490, 1980.

McIver, R.D., Gas hydrates, in *Long-term Energy Resources, vol. 1*, pp. 713-726, edited by Meyer R.F. and J.C. Olson, Pitman, Boston, Mass., 1981.

McIver, R.D., Role of naturally occurring gas hydrates in sediment transport, *AAPG Bull., 66*, 789-792, 1982.

Meyer, R.F., Speculations on oil and gas resources in small fields and unconventional deposits, in *Long-term Energy Resources, vol. 1*, pp. 49-72, edited by Meyer R.F. and J.C. Olson, Pitman, Boston, Mass., 1981.

Osborn, T.J. and T.M.L. Wigley, A simple model for estimating methane concentration and lifetime variations, *Clim. Dyn. 9*, 181-193, 1992.

Paull, C.K., W. Ussler III, and W.P. Dillon, Is the extent of glaciation limited by marine gas-hydrates? *Geophs. Res. Lett. 18*, 432-434, 1991.

Pflaum, R.C., J. M. Brooks, H.B. Cox, M.C. Kennicutt II, and D-D. Sheu, Molecular and isotopic analysis of core gases and gas hydrates, Deep sea drilling project leg 76, in *Initial Reports of the Deep Sea Drilling Project 96*, edited by A.H. Bouma et al., pp. 781-784, U.S. Government Printing Office, Washington, D. C., 1986.

Premuzic, E.T., C.M. Benkovitz, J.S. Gaffney, and J.J. Walsh, The nature and distribution of organic matter in the surface sediments of the world oceans and sea, *Organ. Geochem., 4*, 63-77,1982.

Rasmussen, R.A., M.A.K. Khalil, and F. Morales, Permafrost methane content: Experimental data from sites in northern Alaska, *Chemosphere, 26*, 591-594, 1993.

Revelle, R.R., Methane hydrate in continental slope sediments and increasing atmospheric carbon dioxide, in *Changing Climates*, pp. 252-261, National Academy Press, Washington, D. C., 1983.

Rueff, R.M., and E.D. Sloan, Effect of granular sediment on some thermal properties of tetrahydrofuran, *Ind. Eng. Chem. Proc. Des. Dev. 24*, 882-885, 1985.

Schroter, J.P., R. Koboyashi, and M.A. Hildebrand, Hydrate decomposition conditions in the system H_2S-methane-propane, *Ind. Eng. Chem. Fundam., 22*, 361-364, 1983.

Shipboad Scientific Party, Site 796, in *Proceedings of Ocean Drilling Program, Initial Reports, 127*, pp. 247-322, College Station, Tex., 1990.

Shipley, T.H., and Didyk, B.M., Occurrence of methane hydrates offshore southern Mexico, in *Initial Reports of the Deep Sea Drilling Project 66*, edited by J.S. Wathins, et al., pp. 547-555, U.S. Government Printing Office, Washington, D. C., 1982.

Sloan, E.D., *Clathrate Hydrates of Natural Gases*, 641 pp., Marcel Dekker, New York, 1990.

Trofimuk, A.A., N.V. Cherskiy, and V.P. Tsarev, The role of continental glaciation and hydrate formation on petroleum occurrence, in *Future Supply of Nature-Made Petroleum and Gas*, pp. 919-926, Pergamon, New York, 1977.

Tucholke, B.E., G.M. Bryan, and J.I. Ewing, Gas-hydrate horizons detected in seismic-profiler data from the western North Atlantic, *Am. Assoc. Petr. Geol. Bull., 61*, 698-707, 1977.

Vysniauskas, A., and P.R. Bishnoi, Thermodynamics and kinetics of gas hydrate formation, in *Natural Gas Hydrates: Properties, Occurrence and Recovery*, edited by Butterworth, pp. 35-48, Stonham, Mss., 1983.

Ward, B.B., K.A. Kilpatrick, P.C. Novelli, and M.I. Scranton, Methane oxidation and methane fluxes in the ocean surface layer and deep anoxic waters, *Nature, 327*, 226-229, 1987.

Ward, B.B., K.A. Kilpatrick, A.E. Wopat, E.C. Minnich, and M.E. Lidstrom, Methane oxidation in Saanich Inlet during summer stratification, *Cont. Shelf. Res., 9*, 65-75, 1989.

Whalen, S.C., and W.S. Reeburgh, Consumption of atmospheric methane by tundra soils, *Nature, 346*, 160-162, 1990.

Whiting, G.J., and Chanton, J.P., Primary production control of methane emission from wetlands, *Nature 364*, 794-795, 1993.

Yefremova, A.G., and B.P. Zhizhchenko, Occurrence of crystal hydrates of gases in the sediments of modern marine basins, *Dokl. Acad. Sci. USSR Earth Sci. Sect., 214*, 219-220, 1975.

L.D.D. Harvey, Department of Geography, University of Toronto, 100 St. George Street, Toronto, Canada M5S 1A1. (e-mail: harvey@geog.utoronto.ca)

Z. Huang, Chinese Academy of Sciences, Institute of Atmospheric Physics, Beijing, China 100029.

(Received June 21, 1993; revised July 8, 1994;
accepted October 28, 1994.)